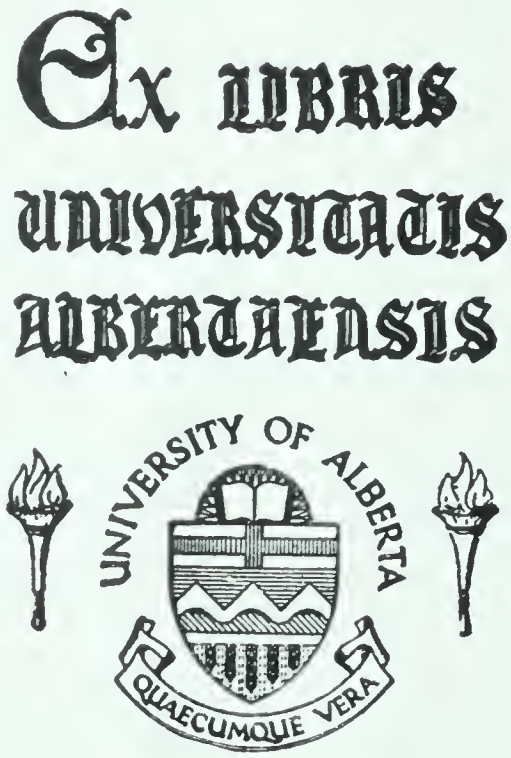


*University of Alberta*
*Printing Department*

THE UNIVERSITY OF ALBERTA

# MICROSEISMS IN ALBERTA

by

Erik Hjortenberg

A THESIS

SUBMITTED TO THE FACULTY OF GRADUATE STUDIES

IN PARTIAL FULFILMENT OF THE REQUIREMENTS FOR THE DEGREE

OF DOCTOR OF PHILOSOPHY

DEPARTMENT OF PHYSICS

Edmonton, Alberta

November, 1963
1964.

THE UNIVERSITY OF ALBERTA

FACULTY OF GRADUATE STUDIES

The undersigned certify that they have read, and recommend to the Faculty of Graduate Studies for acceptance, a thesis entitled MICROSEISMS IN ALBERTA, submitted by Erik Hjortenberg in partial fulfilment of the requirements for the degree of Doctor of Philosophy.

## ABSTRACT

This thesis describes various aspects of the origin and nature of microseisms, in the light of experimental work and measurements made in Alberta during 1962 and 1963.

Microseisms of two different ranges are studied: 3 to 10 seconds and 2 to 50 cycles per second. The latter range is divided into the 3 cps anomalous peak and the 4 - 50 cps microseisms.

The 3 - 10 second microseisms were recorded at the University of Alberta Seismic Observatory at Edmonton during July and August 1963. Directions of approach are determined for microseismic storms and they are compared with the weather situation. It is concluded that 3 - 5 second microseisms of Pacific origin are very heavily damped, so that a barrier for such microseisms exists. The barrier will possibly also act on 5 - 6 second microseisms, but the 8 second microseisms of Pacific origin are well recorded.

The general agreement between the periods observed and those predicted from Longuet-Higgins' theory adds more support to this theory, which is accepted by some but not by all seismologists.

A peak of energy at 3 cps is often found in Alberta, and it is shown that trains, heavy trucks, and farm machinery are effective sources for such microseisms.

The attenuation and the nature of the waves are studied. In some cases retrograde motion is dominant; in other cases pure prograde motion occurs consistently. This suggests the occurrence of both $M_1$ and $M_2$ waves in the 3 cps microseisms.

A clear daily variation of 2-3 cps microseisms is demonstrated and it is shown, that this is not due to variation of wind; other causes are discussed.

Microseisms of frequencies 7 and 12 cps show consistent prograde particle motion in some cases, but consistent retrograde particle motion in others.

In the Appendix a general discussion of Rayleigh type waves in a two layer case is given. It is shown that Rayleigh's constant can be used as an exploration tool, as suggested by Lee.

ACKNOWLEDGEMENTS

The data used for the preparation of this thesis are some recordings made by the modern seismic equipment, acquired by the University of Alberta during the past few years.

The author is indebted to his two successive supervisors Prof. G. D. Garland and Prof. G. L. Cumming, and to Prof. K. Vozoff for valuable advice, interesting discussions on the subject and for permission to use a recording truck and various seismic instruments.

The research during the summer months of 1962 and 1963 was supported by the Advanced Research Projects Agency - Project Vela Uniform, and the author is very grateful for this support. Furthermore he wishes to express his gratitude to the National Research Council for the opportunity of attending the IUGG meeting in Berkeley.

The personal communications in this thesis originate from that meeting, and he wishes to thank the contributors: Prof. P. L. Gouin, Mr. B. Isacks, Dr. J. Oliver, Mr. R. Page, Prof. Y. F. Savarensky, Dr. E. J. Douze and Mr. L. R. Sykes.

Thanks are due to Mr. David Robertson for very helpful assistance during the 1962 field season and for

the supply of records from Lake Superior. Thanks are also due to Miss Helen Hufnagel for the competent typing, to Mr. Gary Kingsep for proofreading the manuscript and to Mr. Bruce McGavin for help and for interest in the problems concerned with the microseisms at the observatory.

TABLE OF CONTENTS

## LIST OF TABLES

LIST OF FIGURES

# I. INTRODUCTION

## 1.1 Historical, Theories on Microseisms

Microseisms are defined as more or less regular ground motion with periods not exceeding a few minutes and continuing with constant or varying amplitude in such a way that they can be assumed not to be caused by earthquakes or explosions. Exploration geophysicists use the term "seismic noise" to designate the high frequency disturbances encountered in their work. They, however, include the shot-generated surface waves, when they are unwanted disturbances on the seismogram. Since the present work deals with ground vibrations generated by sources other than earthquakes and explosions, the term "microseisms" is preferred.

In the nineteenth century microseisms were noticed by astronomers and geodesists, who, using a pool of mercury, rarely found the surface quiet. And Darwin trying to observe the lunar tides in the earth's crust had to abandon the experiment because of ground vibrations.

The term "microseism" was introduced by Bertelli about 1870; he was the first to study the phenomenon systematically, measuring pendulum movements by microscope; and he found that a relationship existed between microseisms and disturbed air-pressure at sea.

After the improvements of seismic instruments

beginning late in the nineteenth century, microseisms attracted the interest of many observers. Wiechert (1905) suggested the surf to be the cause of the observed microseisms, and was supported by Gutenberg (1912 and 1921) who found a strong correlation between microseisms in Göttingen, and waves observed at Norwegian coast stations. He also found that these microseisms may be traced as far away as Siberia.

Through many years the surf theory was the only accepted theory for generation of 3-10 second microseisms; in German it was even called "Brandungsunruhe". However Banerji (1930) noted that in the case of a storm approaching the Indian Ocean, the largest microseisms occurred some hours before the storm reached the coastline. The same result was obtained by Gherzi (1924), who put forward the theory that microseisms are generated by rapid pressure variations in the center of a cyclone. Several objections have been made to this theory: the amplitude of the barometric oscillations seems too small, and the theory does not explain why the cyclone has to be situated over the sea, and why the sea has to be open (not covered with ice).

The latter conditions are satisfied by the surf theory, and to meet Banerji's objection Gutenberg and van Straten (1953) use the term "surf theory" in a broader sense. This means that the new surf theory only states that the wave energy produced by storms radiates through the ocean

in the form of ocean swell until it reaches a continental boundary or the coast, and here by a mechanism not specified in the theory, the disturbance is transmitted to the solid continental block.

Press and Ewing (1948) worked out a mathematical theory for the mechanism of the energy transmission and found that the periods observed in the ordinary microseisms (i.e. 3-10 sec.) could be explained, regarding the system water plus bottom as a single acoustic system giving normal mode propagation with constructive interference, when periods and water depths were subject to certain conditions.

How the oscillations are excited is not quantitatively specified in Press and Ewing's theory. Donn (1957) proposes that the breaking of waves at sea would produce a sufficiently high random noise level, while Longuet-Higgins (1950) develops a mathematical theory, based on Miche's finding that second order pressure variations due to interference of opposing waves can produce microseisms of the required amplitude. The theory predicts a 2:1 ratio of water wave periods and microseism periods and often such ratios have been found. The theory has subsequently been verified in tank experiments. Banerji (1935) shows by tank experiments that pressure variations can be propagated with acoustic speed from a certain plane near the surface ~~and~~ to the bottom. In most treatises on water waves these pressure variations are

ignored, because they do not appear when the usual procedure of dropping second order terms is applied.

The assertion that almost all microseisms in the period spectrum 3-8 seconds are generated by the mechanism of interference of water waves is believed by some and questioned by others, but it may be regarded a good working hypothesis.

Haubrich et al (1963), using a digital seismograph system, find a seismic spectral peak with a frequency which is twice the frequency of the ocean waves as ~~it~~ is expected according to Longuet-Higgins' theory, but they also find a seismic peak of the same frequency as the ocean wave frequency, as expected according to Wiechert's theory (the frequency quoted is 70 millicycles per second). The latter seismic peak has only one per cent of the power which is associated with the first one.

There are different reasons why the microseisms are studied so eagerly; one is that microseisms show many unexplained features like narrow spectra, regular beats or rapidly varying amplitudes. Another reason is that the study of microseisms might make it possible to infer something about parameters of the earth's crust and about atmospheric and oceanographic disturbances. Very often conclusions of this kind have been made in publications concerning a few case histories but very seldom have the results achieved

been generally accepted.

The above discussion is concerned with the 3-10 second microseisms. In recent years, however, the interest in microseisms of higher frequencies has been increasing. This is partly because of the more widespread use of instruments capable of recording higher frequencies, and partly because of the importance of choosing quiet sites for the costly, but efficient observatories using seismic arrays. Moreover, "the study of short period microseisms could become of interest to the earthquake engineers, because E. M. Antonenko (1963) in her studies of microseisms found a close correlation between the amount of old earthquake damage and the amplitude of microseisms in the period range 0.15 to 0.35 seconds", (Y. F. Savarensky, personal communication).

During the last fifteen years, only 13 out of 238 papers on microseisms, abstracted by the U. S. Geological Survey Bulletins,* were concerned with short period (less than one second) microseisms, but in future this ratio is likely to increase. Suggested sources for these microseisms are traffic, machinery, wind and rain (Wilson, 1953a), atmospheric micro-oscillations (Walsh, 1955) and daylight (Gherzi, 1962). Further discussions on short period microseisms follow in chapter 5, together with some results based on the University of Alberta recordings.

---

* Geophysical Abstracts

The main object of the approach made in this thesis is to investigate microseism sources and the nature of the waves. Another approach is made by Galbraith (1963) who treats microseisms from a statistical point of view for the purpose of designing filters that would suppress the microseisms and enhance the seismic signals. The approach in this thesis is to do something with them; Galbraith's approach is to do something about them.

## 1.2 Nature of Microseismic Waves

Numerous authors have found that microseisms contain a large fraction of ordinary Rayleigh waves*; some have even come to the conclusion that all of them are ordinary Rayleigh waves, while in other cases comparable proportions of Rayleigh and Love waves** have been demonstrated. Thus it appears that the vertical component of microseisms has often been assumed to consist entirely of Rayleigh waves and it is only close to the source (Wilson 1953b) that body waves*** have been demonstrated as an additional component. This of course does not exclude the possibility that other kinds of surface waves than ordinary Rayleigh and Love waves could be components of microseisms.

One example demonstrating this possibility was given by Monakhov and Dolbilkina (1958) in an investigation of microseisms at Yalta. Using an ordinary seismograph, an

---

* Surface waves with a longitudinal and a vertical transverse displacement.
** Surface waves with a horizontal transverse displacement.
*** Elastic waves, either longitudinal P waves or transverse S waves.

azimuthal seismograph, a vector seismograph and a tripartite station. When studying individual oscillations of Atlantic origin, they found a complicated particle motion in most of the cases, but a narrow angle of approach was usually pointing towards the Norwegian coast. In seven to twenty-seven per cent of the cases they found pseudo-Rayleigh waves, i.e., waves differing from pure Rayleigh waves only by having a plane of oscillations tilted towards one side, but retaining all other properties of the Rayleigh waves; they found practically no Love waves. It is tempting to suggest that those pseudo-Rayleigh waves are due to interference between pure Rayleigh waves and Love waves because when only a few consecutive oscillations can be studied it seems impossible to distinguish between the two phenomena. However, if Love waves were present they should sometimes occur between the beats of the vertical, and the azimuthal setup would make their identification probable; but no such Love waves were reported. Furthermore, in a large number of samples, the Love waves would be statistically independent of the Rayleigh waves and the apparent angle of inclination should occur on both sides of the vertical with equal probability. However, for most azimuths there appeared to be a strong tendency for the plane of vibration always to tilt to the same side. The angle of tilt was most often twenty to thirty degrees and never exceeded forty-five degrees.

This phenomenon seems unexplainable, using simple horizontal layer models, but may be explainable using a more

complicated crustal model for southern Russia.

An interpretation of these data without recourse to departures from classical elasticity theory can be derived from the discussions given by Oliver and Ewing (1958a) and Jones (1963): They describe Leet's C wave or coupled wave, which has a definition similar to that of the pseudo-Rayleigh wave. They point out that Love waves and Rayleigh waves would arrive almost simultaneously if the travel times of such waves are similar, and they show that a similarity exists between the velocities of $M_2$ continental Rayleigh waves and of the second mode Love wave.

Since pseudo-Rayleigh waves were found to have a fairly small angle of inclination at Yalta, the transverse component of such waves is expected to be smaller than the longitudinal. However, Jensen (1961) found no significant difference between the amplitudes of the longitudinal and transverse component for those eighty-two days in which the microseisms were approaching from the northern octant. This strongly suggests that Love waves are present in the microseisms recorded at Copenhagen, and that their amplitudes are similar to those of the Rayleigh waves. Furthermore, the sinusoidal variation of velocity vectors (Jensen 1958, p. 16) are most likely due to interference of a group of Love waves and a group of Rayleigh waves. It seems improbable that

two simultaneous but entirely different sources should make a regular interference pattern such as was suggested by Båth (1962).

The Rayleigh waves and the pseudo-Rayleigh waves discussed above both have a retrograde particle motion, i.e. motion with a velocity towards the source in the upper portion of the trajectory. The opposite type of particle motion is called prograde, and this particle motion is the same as that exhibited by water waves.

Prograde waves were theoretically predicted by Sezawa and Kanai (1935) by considering the dispersion of Rayleigh waves in a two layer case. The equations resulted in two different dispersion curves, one of them corresponded to the fundamental Rayleigh mode, the other one they called the $M_2$-mode, both modes were considered fundamental because of the absence of nodal planes. They found that the $M_2$-Rayleigh wave (Sezawa wave) had orbital motion opposite that of ordinary Rayleigh waves (i.e., prograde instead of retrograde). Nagamune (1956) found that in a three layer case $M_2$ waves may be either prograde or retrograde.

Oliver and Ewing (1957) pointed out that the calculations of Sezawa and Kanai had led to the general belief that the $M_2$ mode was characterized by prograde (elliptical and progressive) particle motion. In a two

layer case with the low rigidity contrast (1:2.09) pertinent to the problem of higher mode continental Rayleigh waves, however, they found the $M_2$ wave to have retrograde motion for all wave-lengths, and in another case with higher rigidity contrast (1:8), they found the particle motion to change from prograde to retrograde within the same mode.

While $M_2$ waves may have both types of motion, the fundamental mode Rayleigh wave, at least in any realistic, layered model, will always have retrograde particle motion (J. Oliver, personal communication).

In 1955 Kanai ascertained that $M_2$ waves appear only when the velocity in the surface layer is smaller or slightly larger than the velocity in the lower layer and he concluded:

"Moreover, though Sezawa waves cannot be seen when the wave-length exceeds a certain limit, the reason why Sezawa waves are rarer than Rayleigh waves in cases of shorter wave-lengths is hard to find. Also, there is no reason why the amplitude of Sezawa waves is smaller than that of Rayleigh waves, but in some cases, it seems that the amplitude of Sezawa waves becomes larger than that of Rayleigh type waves."

In view of this theoretical prediction it is interesting to note that prograde Rayleigh waves later were found in waves from explosions, as demonstrated by Kisslinger (1959) and

by Jones (1963). They have also been found in microseisms, which will be demonstraded in the present work. No previous demonstration of such Sezawa-type waves in microseisms is known to the writer. It is not very surprising, though, that previous workers have felt justified in the assumption that the vertical component of microseisms was composed of retrograde Rayleigh waves. The reason is that earlier work on particle motion in microseisms has been done on microseisms with periods longer than four seconds, and several investigations suggest that any prograde waves in such microseisms are negligible. One such investigation is the routine determination of the direction of approach in Copenhagen by Jensen's method (Jensen 1959). Here the most frequent direction of approach was from the northern sector, confirming Gutenberg's original work and recent Russian work indicating the Norwegian coast as a prominent source area. However, if the microseisms had contained an appreciable amount of prograde $M_2$ waves, a number of directions should group around the antipole, i.e., in the southern sector, and no such tendency occurred.

Another investigation made by Oliver and Ewing (1957) led to the same result. They demonstrated theoretically (as mentioned before) and experimentally (investigating an Arctic earthquake) that the $M_2$ particle motion is retrograde in a continental crust. The microseisms in which prograde particle motions were observed at the

University of Alberta were of periods shorter than half a second.

Some additional information about Rayleigh-type waves in a two layer model is given in Appendix A.

# II. METHODS OF INVESTIGATIONS

## 2.1 Procedure for Investigating the Nature of Microseismic Waves

Jensen's method (see page 28) is a method for determining the direction of approach, given the assumption that Rayleigh waves are present; the same method will be used here for determining the nature of waves assuming that the direction of approach is known. Since the purpose thus is modified, it could be called the modified Jensen method.

The first concern of this method is knowledge of the source. In some cases, particularly in artificial noise, the source can be established beyond any doubt. In such cases the direction of approach will most often be the direction to the source, but some lateral refraction may occur on the path. A safer method is therefore to use an L-spread of geophones to determine the direction of approach right on the site, where the waves are analyzed. In addition to this a three-dimensional registration must be made: one vertical (Z), and two horizontals, usually N and E, all recorded at the same location. The three components should preferably have the same responses. If that is the case the procedure is to select times where Z is maximum and measure dN/dt and dE/dt and plot these points in a NE diagram. In the same diagram the vector pointing towards the source and the line

through the origin perpendicular to this line are drawn.

Now the distribution of points obtained is compared with the cases shown in Figure 1, and it may be possible to decide which case is appropriate. If small amounts of extraneous microseisms are present the scatter may be increased somewhat, and if larger amounts are present it may be necessary to use statistical methods on a large number of determinations before any conclusions can be drawn, as shown by Jensen (1961). If in cases (b) and (c) Rayleigh waves and Love waves have constant amplitudes of similar magnitudes the points would scatter in a quarter plane, but due to the amplitude modulations usually present in microseisms, they will scatter in a half plane as shown in Figure 1.

## 2.2 Procedure for Determination of the Direction of Approach by Wave Correlation in an L-Spread

When three or more suitably spaced geophones are laid out to form a right angle or a cross, it is possible to determine the direction of approach, provided that a substantial part of the waves in a fairly narrow frequency range have their directions of approach in a fairly narrow sector. Successes of the tripartite method have been obtained when this condition was satisfied, and failures have resulted in cases when it was not satisfied. When the condition is not satisfied, it is sometimes possible to identify waves

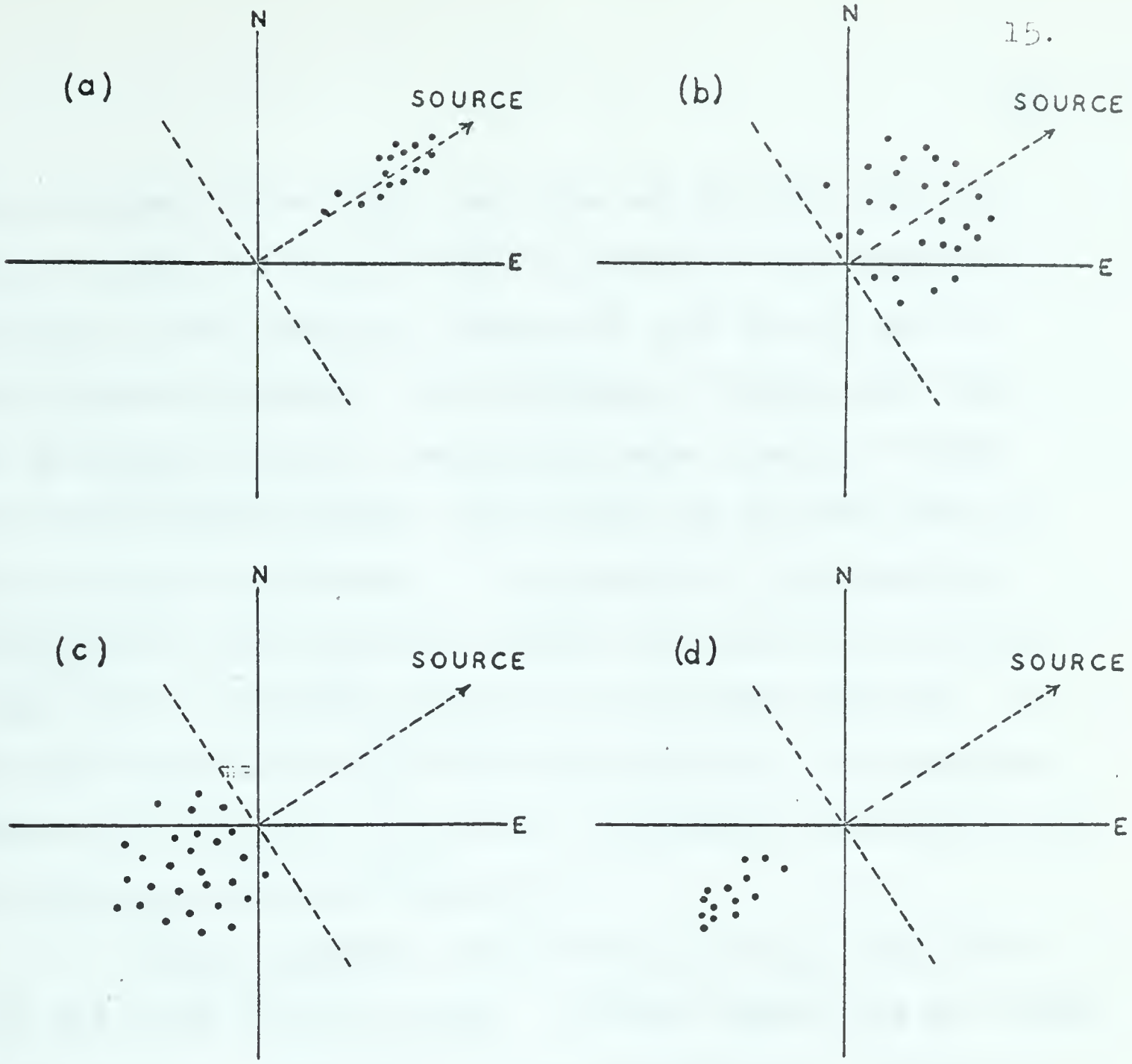


Possible nature of surface waves, when only one source is present:

(a) $M_1$ .Rayleigh waves ( ordinary Rayleigh waves )

(b) $M_1$ Rayleigh waves and Love waves

(c) $M_2$ Rayleigh waves and Love waves

(d) $M_2$ Rayleigh waves ( Sezawa waves )

Points plotted are $\left(\frac{dN}{dt}, \frac{dE}{dt}\right)$ read at times where Z is maximum

( ARTIFICIAL EXAMPLE )

FIG. 1.

from different directions, and this can be done with much better chances of success when a spread of many geophones is used in each direction instead of just two as used in the tripartite method. The advantage of having more than two geophones is that a propagating wave crest or trough will show a clear lineup, which often can be identified on top of other disturbances. One example of a mathematical evaluation of the tripartite method was given by Gutenberg (1958) for an arbitrary location of the three stations. In the text below a simpler method is evaluated, which applies when it is possible to determine the apparent velocity in two mutually perpendicular directions.

Assume apparent velocities $V_N$ and $V_E$ along a NS line and an EW line are known. Positive directions are taken to be N and E. Consider a wave propagating in a direction determined by the vector $\hat{v}$. Let $|\hat{v}| = v$. Let $\hat{n}$ and $\hat{e}$ be unit vectors pointing toward N and E. The angle between $\hat{n}$ and $(-\hat{v})$ is called $\alpha$, i.e., $\alpha$ is the azimuth of the direction of approach. Let $\alpha$ be positive in the two eastern quadrants and negative in the two western quadrants, $-180^\circ < \alpha \leqslant 180^\circ$. Consider a point moving with the wave in the direction $\hat{v}$. The velocity of its projection on a meridian is then $\hat{v} \cdot \hat{n}$, positive if moving north, and the velocity of its projection on a parallel is $\hat{v} \cdot \hat{e}$ positive if moving east. $v_N$ has the same sign as $\hat{v} \cdot \hat{n}$ and hence (Figure 2)

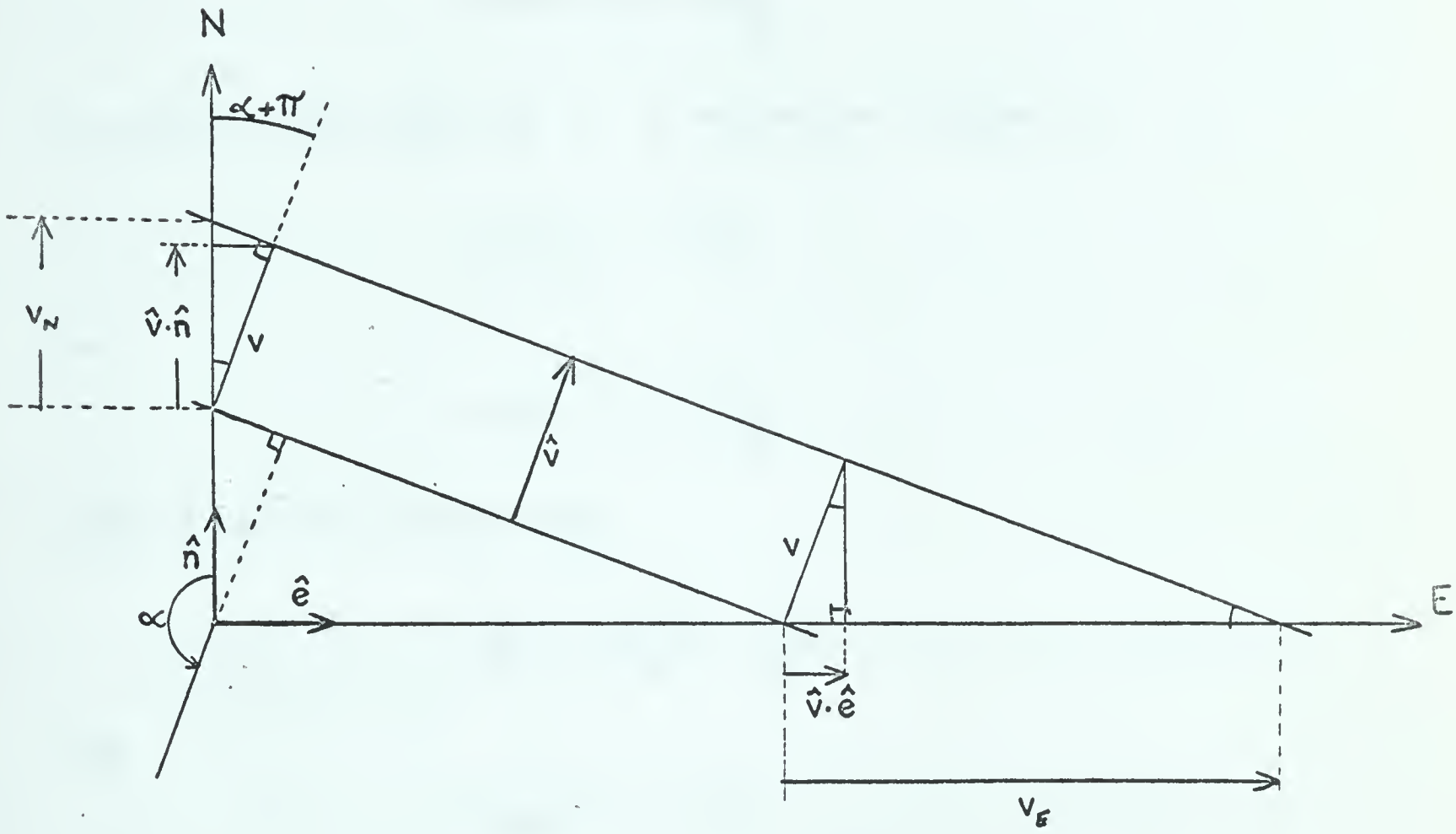


$\alpha$ : Direction of approach

$\hat{v}$ : Direction of wave propagation

$v=|\hat{v}|$ : Velocity of wave propagation

$v_N$ : Apparent velocity in SN-direction

$v_E$ : Apparent velocity in WE-direction

Determination of the direction of approach from the apparent wave velocity in an L spread.

FIG. 2.

$$\frac{v}{\hat{v} \cdot \hat{n}} = \frac{V_N}{v}$$

or

$$\cos \alpha = - \frac{V}{V_N}$$

$V_E$ has the same sign as $\hat{v} \cdot \hat{e}$ and hence (Figure 2)

$$\frac{v}{\hat{v} \cdot \hat{e}} = \frac{V_E}{v}$$

or

$$\sin \alpha = - \frac{V}{V_E}$$

from which it follows that

$$\frac{1}{V^2} = \frac{1}{V_N^2} + \frac{1}{V_E^2}$$

and

$$\tan \alpha = \frac{V_E}{V_N}$$

As shown by Longuet-Higgins (1957) the relations are simpler when vectorial wave numbers are used.

$(W_N, W_E) = \hat{w} = \frac{\hat{v}}{v^2} = \overrightarrow{OP}$ is the vectorial wave number

$$|\hat{w}| = \frac{1}{v}$$

$\frac{1}{V_N} = W_N$ is the wave number in the N-direction

$\frac{1}{V_E} = W_E$ is the wave number in the E-direction

Wave number in a direction given by the unit vector $\hat{m}$ is $\hat{w} \cdot \hat{m}$.

If several waves are present simultaneously with wave numbers $OP_n$ which are slightly different, then the wave number determined from the L-spread will be the center of mass of the points $P_n$, each weighted by the corresponding component amplitude. In that case the velocity determined is the average phase velocity, but as was pointed out by Jones (1963 and personal communication) the differences between the component wave numbers (and hence frequencies) must be so small that their differences only contribute to the shape of the envelope (the modulation) without too much distortion of the carrier frequency.

## 2.3 Procedure for Measurement of Amplitudes and Frequencies of Microseisms

Most often microseisms show a beat phenomenon, and irregular microseisms are often made up of different more regular components each of which shows beats, so that each component frequency may show up as a sinusoidal train of waves between beats of other frequencies. It is thus possible to measure some component frequencies by visual observation, and if the recording is not made on magnetic tape, suitable for automatic power spectrum analysis, a fairly accurate measure of the power associated with a certain frequency can be obtained by taking the average of several typical beat maximum amplitudes. This yields an estimate somewhat larger than

the average amplitude (in the mean square sense), but it is an estimate that according to practical experience and theoretical considerations doesn't vary too much as long as the source conditions remain constant.

Such theoretical considerations were given by Longuet-Higgins (Vesiac Staff, 1962, Chapter 8), who defines a parameter $\epsilon$ related to the narrowness of the spectrum. An estimate of $\epsilon$ is given by

$$\epsilon^2 \simeq \frac{(N_o^1)^2 - (N_o)^2}{(N_o^1)^2} \qquad (2\text{-}1)$$

where $N_o$ is the number of zero up crossings

$N_o^1$ is the number of crests

in some length of the record.

When $\epsilon = o$ the median of the distribution of the maximum crest amplitudes in a random sample of N crests will be 2.9 times the root mean square amplitude at N = 64 and 3.4 times rms amplitude at N = 256. The corresponding 10 percent fractiles are 2.6 and 3.1, i.e., the ratio between maximum crest and rms amplitude will usually be around 3. This is for gaussian noise with $\epsilon = o$, but also for gaussian noise with $\epsilon = 0.9$ the ratio will be around 3 for a reasonably-sized sample. A reason for not choosing larger samples is that the condition of statistical stationarity is not often fulfilled in a sample larger than a few hundred.

Figure 3 shows the cumulative probability distributions of a quantity x, which is the maximum crest amplitude divided by the rms amplitude, in a sample of N crests, for $N = 2^0, 2^1, \ldots\ldots, 2^{15}$; (taken from Cartwright, 1958).

The value obtained by this procedure will thus be approximately three times the rms amplitude for gaussian noise. When gaussian noise has a prominent and fairly narrow spectrum (most of the energy within one octave) it is possible by visual observation to obtain the mean frequency of this power density peak. This was shown by Rice (1944, 1954) who proved that the mean number of zeros per second is

$$2 \left[ \frac{m_2}{m_o} \right]^{1/2} \qquad (2\text{-}2)$$

where the moments $m_n$ of the spectrum are defined:

$$m_n = \int_o^\infty w(f) f^n df \qquad (2\text{-}3)$$

$w(f)$ being the power density associated with the frequency f. For $n = 0$

$$m_o = \int_o^\infty w(f) df = \lim_{T \to \infty} \frac{1}{2T} \int_{-T}^{T} [y(t)]^2 \, dt \qquad (2\text{-}4)$$

where $y(t)$ is the ground amplitude measured from its mean level. $\sqrt{m_o}$ is the rms value of the amplitudes.

The interpretation of $w(f)$ as power density requires a little clarification. For frequencies between f and f + df

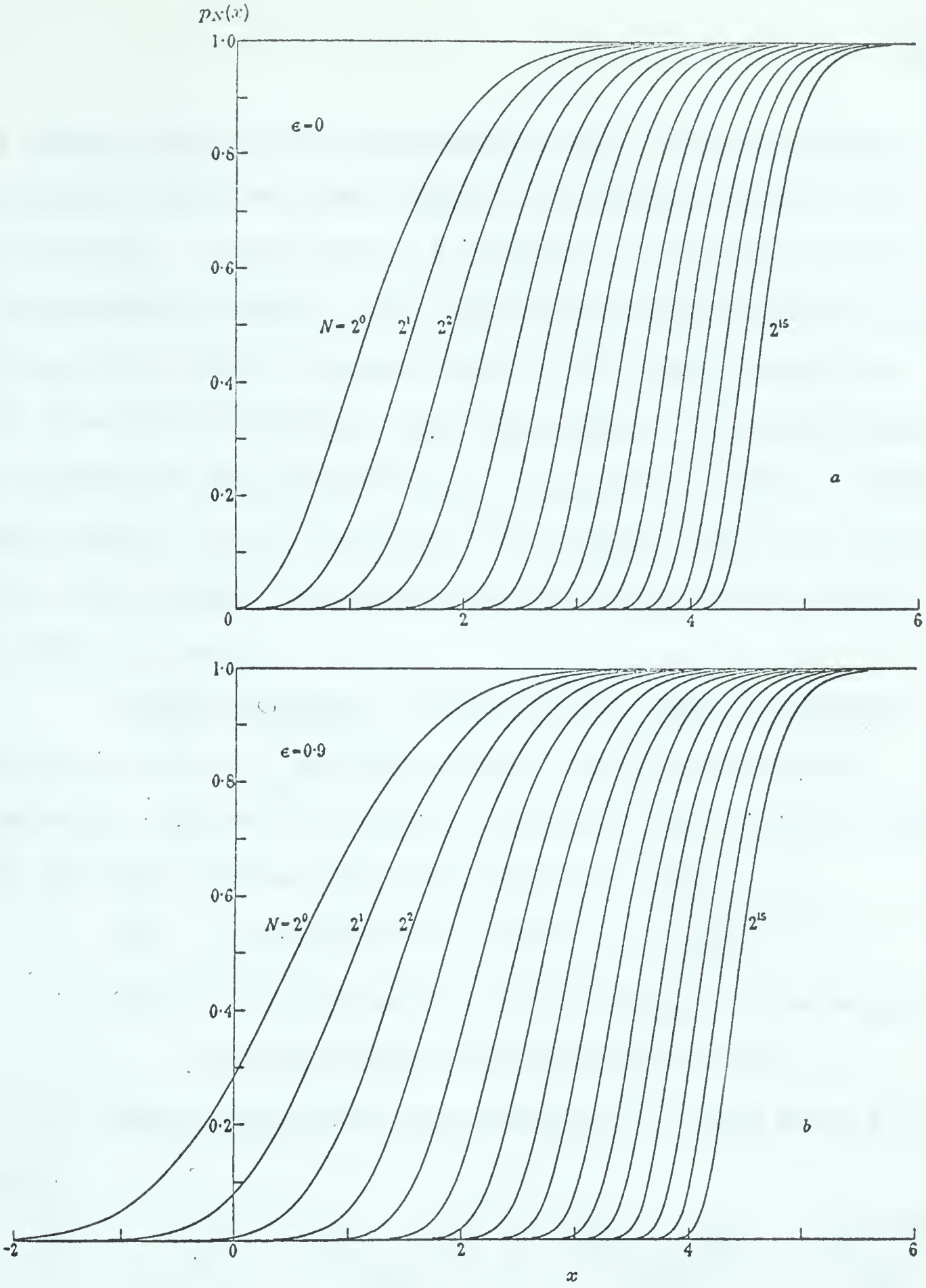


FIGURES 1 *a* and *b*. Probability functions $p_N(x)$ (equations (1) and (4)) for various values of $N = 2^m$ and (*a*) $\epsilon = 0$, (*b*) $\epsilon = 0{\cdot}9$.

*After Cartwright (1958)*

FIG. 3.

Probability functions for the amplitude of the highest of N crests.

the power output of the seismometer will be proportional to w(f)df, with the same constant of proportionality for any location. Thus w(f) is a measure of the power density of seismometer output. For stationary surface waves w(f)df and hence $m_o$ will be proportional to the mean energy per unit area of the surface, but the constant of proportionality will depend on the properties of the ground. Thus a larger power density on one location than another does not necessarily mean larger ground energy; if the ground is softer it may even be lower.

Longuet-Higgins (Vesiac staff, 1962, Chapter 8) pointed out that in gaussian noise the distribution of intervals $\tau$ between successive zeros has the following properties when the narrow band approximation holds:

a) It is symmetrical about $\tau = \frac{1}{2}(\frac{m_o}{m_2})^{1/2}$

b) It is independent of the shape of the original spectrum except for its rms width $\delta$

The narrow band approximation is valid when $\delta << 1$ where:

$$\delta^2 = \frac{m_2 m_o - m_1^2}{m_2 m_o} = \frac{\overline{(f^2)} - (\bar{f})^2}{\overline{(f^2)}} = \frac{\overline{(f - \bar{f})^2}}{\overline{(f^2)}} \qquad (2\text{-}5)$$

it holds when most of the energy is within one octave or less.

If the energy is divided between two or more power density peaks more than an octave apart, the shorter periods will clearly show up superimposed on the longer ones, and each kind of microseism may be analyzed separately from the same record.

Thus for an analogue record it is possible to determine the mean frequency by simply taking the mean of zero-crossover intervals at randomly-distributed times. When $\epsilon = 0$, which is often the case, the interval between successive crests will simply be twice the interval between successive zeros. When $\epsilon > 0$, the distribution of crests will involve the moment of fourth order (Vesiac Staff, 1962, Chapter 8). According to the same source the empirical distribution of zero-crossover intervals will also depend on the width of the spectrum, so that the interquartile range of this distribution will be equal to $[2/\sqrt{3}](\delta\bar{\tau})$. By estimating the interquartile range it is thus possible to form an estimate of $\delta$, the rms width of the spectrum per unit of frequency.

If more knowledge of the shape of a spectral peak is required, or if resolution of two closely-spaced spectral peaks is essential, digitizing the record is required, in order to calculate the power spectrum.

## 2.4 Procedure for Determination of the Attenuation of Microseisms

When the term "attenuation of seismic waves" is used, it means the decrease of amplitude, which theoretically is due to conversion of elastic energy to heat, but in practice scattering and reflections may account for a portion of the attenuation. At any rate the attenuation will be zero, in a perfectly elastic, homogeneous medium. Bullen (1953) prefers the word damping, meaning precisely the same as what other authors would call attenuation.

Since microseisms consist primarily of surface waves, it is reasonable to define attenuation of microseisms with reference to Rayleigh waves in a homogeneous, isotropic, perfectly elastic halfspace. For such a halfspace Rayleigh waves from an infinite line source would have a constant amplitude as a function of distance. Rayleigh waves from a point source, with harmonic motion proportional to $e^{i\omega t}$, however, would have the following vertical amplitude (Ewing, Jardetzky and Press, 1957, page 40):

$$w_o = ck_\beta^2 \nu_R J_o(kr) \qquad (2\text{-}6)$$

where

$$\nu_R = k^2 - k_\alpha^2$$

$$k_\alpha = \frac{\omega}{\alpha}$$

$$k_\beta = \frac{\omega}{\beta}$$

$$k = \frac{\omega}{c_R}$$

and the constants $\alpha$, $\beta$, $C_R$ are the velocities of P, S and Rayleigh waves respectively, and $\omega = 2\pi f$.

The Bessel function in (2-6) is the only factor that depends on distance. When kr is large enough $J_o(kr)$ will approximate a sine wave with constant wave number k. This result follows from the approximation formula (Gray and Mathews, 1895):

$$J_o(x) \simeq \left(\frac{2}{\pi x}\right)^{1/2} M \cos\left(x - \frac{\pi}{4} - \psi\right) \qquad (2\text{-}7)$$

where

$$M = 1 - \frac{1}{16x^2} + \frac{53}{512x^4} - \ldots\ldots$$

$$\psi = \tan^{-1}\left(\frac{1}{8x} - \frac{33}{512x^3} + \ldots.\right)$$

It also follows that when r is large the amplitude of the Rayleigh wave will be:

$$A = Br^{-1/2} \qquad (2\text{-}8)$$

where the factor $B = Ck_\beta^2 \nu_R \cdot \sqrt{\frac{2}{\pi}}$ is independent of r.

In a medium where attentuation occurs (2-8) will be modified into:

$$A = B \cdot r^{-1/2} \cdot e^{-\alpha r} \qquad (2\text{-}9)$$

and $\alpha$ may be called the attenuation coefficient. Kisslinger (Jones, 1963) found $\alpha$ to vary from 4 to 6 $km^{-1}$ in the range 3.5 to 5 cps. Wilson (1953b) found $\alpha = 1.09$ $km^{-1}$ at 9 cps.

Knopoff and MacDonald (1958) defined the specific dissipation function $1/Q$ such that $2\pi/Q$ is the ratio of energy dissipated per cycle to the energy stored. For a plane propagating elastic wave they found:

$$\frac{1}{Q} = \frac{2\alpha c}{\omega} \qquad (2\text{-}9.1)$$

where c is the velocity of propagation.

Knopoff (1959) quoted two different models for the attenuation:

1. The "Q" or solid friction model, that predicts Q to be independent of the frequency f, and hence the attenuation coefficient $\alpha$ to be proportional to f.
2. The internal friction model, that predicts Q to be proportional to f and $\alpha$ to be proportional to $f^2$.

Knopoff and MacDonald (1958) quote evidence from many sources that the "Q" model applies for most materials at seismic and acoustic frequencies, and it may be expected to apply for most homogeneous materials.

Willis and Wilson (1960) found $Q_R = 140 - 152$ valid for 1 cps Rayleigh-type waves observed 100 - 1000 km from explosive sources. This agrees with the range Q = 100 - 250 given by Knopoff (1959).

Brune (1962) quoted Q = 170 for Rayleigh waves with period T = 140 - 215 seconds and Q = 350 for T = 250 - 350 seconds. He concluded that for dispersive

wave trains the equation (2-9.1) is still valid, provided that c is interpreted as the group velocity. He also concluded that measured values of Q usually reflect the combined loss of energy due to internal friction and scattering.

If an attenuation study is carried out using a comparatively small number of observations, it is necessary to check that the source conditions remain constant. Even if the source is an explosion of the same size in the same shot hole, the energy coupling may have changed at the source.

Sometimes the surface amplitude of seismic signals shows a clear variation from one place to another. For instance earthquake damage will be larger on loose sediments than on solid rock. Consequently in an attenuation study, it must be considered that amplitude differences could be due to such an effect.

A detailed example of an experimental determination of an attenuation coefficient and a discussion of Q values for short period surface waves is given in section 5.3c.

## 2.5 Jensen's Method for the Determination of the Direction of Approach of Rayleigh Waves

A convenient method to apply on photographic records from a homogeneous set of instruments is the Jensen method. The first part of this section will contain an outline of this method, while the later parts will show some new theoretical work, which the author found pertinent to the interpretation of some results achieved by the Jensen method.

## 2.5a Short Outline of Jensen's Method

Jensen's method or the method of the empty half plane has been described by Jensen (1958 and 1961) using vectors and by Båth (1962) using Cartesian coordinates.

Basic Assumptions:

1) Retrograde Rayleigh waves from a single direction are present and they dominate over any other wavetype with a vertical (Z) component.
2) Any other wavetypes contained in the movement are statistically independent of these Rayleigh waves at the times when Z is at a maximum.

Theory:

At the times when Z is at a maximum the retrograde Rayleigh component will contribute to the particle velocity by a vector $\vec{V}_R$ pointing towards the source. A Love wave not correlated with the Rayleigh wave will contribute to the particle velocity by a vector in one of the directions perpendicular to $\vec{V}_R$, but it will assume these two directions with equal probability. The total effect of these two components will be that all the end points of the velocity vectors scatter in the half plane towards the source. An addition of other wavetypes and isotropic noise, uncorrelated with the Rayleigh component will not destroy the tendency of these points to choose the half plane towards the source.

Procedure:

1. Times of well-developed maxima on Z are determined.
2. The slopes $\frac{dN}{dt}$ and $\frac{dE}{dt}$ are measured at these times.
3. The points $(\frac{dN}{dt}, \frac{dE}{dt})$ are plotted in an NE-diagram.
4. Now the vector $(\Sigma \frac{dN}{dt}, \Sigma \frac{dE}{dt})$ is an estimate of the direction of approach.
5. The perpendicular to this vector through origin is drawn and the number r of points in the half plane containing the vector (the "right" half plane) and the number of points w in the other half plane (the "wrong" half plane) are counted.
6. The reliability measure p is determined by the formula

$$p = \frac{r-w}{n} \cdot 10 \qquad (2\text{-}10)$$

where n is the total number of points. An approximate value of the probable error of the direction of approach for positive p values is

$$e = 30 - \frac{5}{2} p \qquad (2\text{-}11)$$

where e is the probable error in degrees (Jensen 1961).

## 2.5b Definition and Interpretation of $A_R$

To make use not only of the direction of the vector $(\Sigma \frac{dN}{dt}, \Sigma \frac{dE}{dt})$ quoted in the previous sub-section, but also of its absolute value, it was found convenient to introduce a quantity $A_R$ defined by

$$A_R = \frac{Ts[(\Sigma \frac{dN}{dx})^2 + (\Sigma \frac{dE}{dx})^2]^{1/2} \cdot 0.798}{2\pi n \, M(T)} \qquad (2\text{-}12)$$

where $T$ = period

$s$ = paper speed

$x$ = distance along recorded trace

$M(T)$ = magnification at period T.

$A_R$ is easy to calculate during the normal procedure. We shall show that this quantity is related to the root mean square horizontal amplitude of the Rayleigh waves:

Assume that all vertical motion is due to Rayleigh waves coming from a single direction. Then Love waves will not contribute to $A_R$ and

$$\frac{A_R}{0.798} \qquad (2\text{-}13)$$

will be an estimate of the mean amplitude of the envelope of the Rayleigh wave. This could yield an estimate a little too large since a small crest will rarely occur among the "well developed" crests mentioned in the procedure.

The time interval used for the determination of the direction of approach is short, and hence according to Longuet-Higgins (Vesiac Staff, 1962, chapter 8) the microseisms in general and the Rayleigh wave in particular can be treated as gaussian noise, and hence (loc. cit.) the quantity

$$\eta = \frac{\text{height of crest (from mean level)}}{\text{root mean square amplitude}} \qquad (2.14)$$

will for $\epsilon = 0$, i.e. for equal number of zero up crossings and crests, follow a Rayleigh distribution. Hence the mean value of the envelope will be

$$\int_0^\infty \eta^2 \, e^{-(\eta^2/2)} \, d\eta = \frac{1}{2} (2\pi)^{1/2} \simeq \frac{1}{0.798} \qquad (2.15)$$

and now it follows from (2-13), (2-14) and (2-15) that $A_R$ will be an estimate of the root mean square horizontal Rayleigh amplitude.

If $A_R$ is small compared with the vertical rms amplitude, the p can also be expected to be small, and such an observation can be explained by assuming that a substantial portion of the vertical amplitude is due to isotropic microseisms; an alternate explanation is that Rayleigh waves are coming in from two directions approximately 180° apart.

2.5c Reliability of small p's

The formula (2-11) gives information about the probable errors as determined by an empirical method (Jensen, 1958, p. 8), but it does not state the probability distribution of errors. If a realistic model for the method is used, the mathematical problems of determining this probability distribution are very involved.

A simple model was chosen, however, for the purpose of determining which p's to expect from a random distribution of points. For the model 21 points are considered, while the number of points used in actual practice often exceeded 21 (see Table III).

The model is this: 21 Bernoulli trials are made with probability $\frac{1}{2}$ for "success". If the number of "successes", $s_n$, exceeds 10, they correspond to points falling in the "right" half plane; then

$$q = \left| \frac{[s_n - (21-s_n)] \cdot 10}{21} \right| \qquad (2\text{-}16)$$

will correspond to the p defined in (2-10).

If the number of "successes" is 10 or less they correspond to points in the "wrong" half plane and (2-16) will still correspond to equation (2-10).

The q's defined here are always positive, and they are generated by a process which has some similarity with the positive p's obtained by applying Jensen's method to slopes measured at random times, rejecting all the determinations with $p \leqslant 0$.

To get information about the probability distribution of q we will apply the de Moivre-Laplace limit theorem (Feller, 1950, p. 137) which for the present purpose yields a good approximation:

$$Pr\ (\alpha \leqslant s_n \leqslant \beta) \simeq \Phi(x_{\beta+1/2}) - \Phi(x_{\alpha-1/2}) \qquad (2\text{-}17)$$

In the present case

$$h = (npq)^{-1/2} = (21 \cdot \tfrac{1}{2} \cdot \tfrac{1}{2})^{-1/2} \simeq 0.436 \qquad (2\text{-}18)$$

$$x_t = (t\text{-}np)h = (t\text{-}10.5) \cdot 0.436 \qquad (2\text{-}19)$$

Hence

$$P_r(q \leqslant \tfrac{30}{21}) = P_r(9 \leqslant s_n \leqslant 12) = 2[\Phi(0.872) - \tfrac{1}{2}] \simeq 0.61 \qquad (2\text{-}20)$$

or $q > 1.4$, i.e. $q \geqslant 2.4$ in 39% of the cases. Similarly we get

$q > 3.3$, i.e. $q \geqslant 4.3$ in 8% of the cases.

$q > 5.2$, i.e. $q \geqslant 6.2$ in 0.9% of the cases.

If p is equal to 6 or larger, it is for practical purposes possible to conclude that the noise is not isotropic. If two determinations with $p \geqslant 6$ give the same result within the limits of accuracy it is possible to infer with complete confidence, that this is a direction of approach, provided that the basic assumptions of the method are satisfied. When $p \leqslant 3$ no conclusion can be made from a single determination, but the distribution of such directions gives a reliable picture of the most frequent directions of approach. As indicated by the probable error the result is often quite good for very small p's, which shows that isotropic noise is not a common phenomenon.

# III. INSTRUMENTATION

## 3.1 Short Description of the Instruments Used

The data used in the preparation of the present thesis are recorded partly by the University of Alberta observatory instruments, and partly by the portable Texas Very Low Frequency Refraction System.

The University of Alberta observatory instruments were installed in the spring of 1962 and were adjusted to standard frequency response and calibrated by Mr. F. Lombardo, Dominion Observatory, using a Willmore bridge. The instruments consist of two sets, a long period and a short period set. The long period set is a homogeneous, three component set of Press-Ewing instruments, manufactured by Lehner and Griffith, having the period of seismometers adjusted to 30 seconds and the period of the galvanometers to 90 seconds. The short period set consists of three Willmore seismometers, two horizontal Mark I and one vertical Mark II used with 1/4 second galvanometers. All the components are recording on Lehner and Griffith triplet recorders which usually eliminates any need of making corrections when comparing two components of a set.

Two identical sets of VLF portable seismic recording equipment were available. One of these sets was used by the author for studying particle motion in short-period microseisms. The equipment was installed in a panel truck,

was run on 12 volt batteries and it consisted of a 100 volt power supply, a 12 channel amplifier bank with adjustable attenuation and high cut filters, a RS-8U camera and 12 vertical seismometers (2 cps). All this equipment was manufactured by Texas Instruments. Two Willmore Mark I seismometers (1 cps) were used for recording horizontal motion. Three cables with 4 take-outs on each made simultaneous recordingson a one mile spread possible. A more detailed discussion of the field equipment is given in the manuals and by Weaver (1962) who also describes some of the problems that arose with the equipment during the first field season.

## 3.2 Determination of Phase and Amplitude Response of the Field Instruments

During the field season 1962 it was impossible to obtain a homogeneous set of instruments, but two horizontal Willmores with periods of one second could be set up and compared with a vertical S-36 Texas seismometer, with a period of one-half second. Thus a knowledge of the phase difference between Willmore and Texas seismometer outputs is necessary in order to apply the modified Jensen method. In order to determine this phase difference for simple harmonic ground motion, let

$$y = y_o + a \sin \omega t \qquad (3\text{-}1)$$

be the coordinate in the direction of recorded motion of a point of the frame (ground), let x be the coordinate of a point of the seismometer mass and let

$$(y - y_o) - (x - x_o) = u \qquad (3\text{-}2)$$

Then $$u = b \sin(\omega t - \delta) \qquad (3\text{-}3)$$

where $\delta$ is the phase angle by which the relative motion of the ground with respect to the seismometer mass lags behind the true ground motion.

Let the force acting on the mass M be $Pu + R\dot{u}$.

Let $\frac{P}{M} = n^2 \qquad \frac{R}{M} = 2\lambda \qquad \frac{\lambda}{n} = h$

Then the equation of motion is

$$\ddot{u} + 2\lambda\dot{u} + n^2 u = \ddot{y} \qquad (3\text{-}4)$$

Now from (3-1) (3-3) and (3-4):

$$b(n^2-\omega^2) \sin(\omega t-\delta) + 2\lambda b\omega \cos(\omega t-\delta) = a\omega^2 \sin \omega t \qquad (3\text{-}5)$$

For the three particular values $t = \frac{\delta}{\omega}$, $t = \frac{\delta}{\omega} + \frac{\pi}{2\omega}$

and $t = 0$ the equation (3-5) reduces to

$$\sin \delta = \frac{2\lambda}{\omega} \cdot \frac{b}{a} \qquad (3\text{-}6)$$

$$\cos \delta = \frac{n^2-\omega^2}{\omega^2} \cdot \frac{b}{a} \qquad (3\text{-}7)$$

$$\tan \delta = \frac{2\lambda\omega}{n^2-\omega^2} \qquad (3\text{-}8)$$

respectively. Now from (3-6) and (3-7):

$$\left(\frac{b}{a}\right)^2 = \frac{\omega^2}{(n^2-\omega^2)^2 + 4\lambda^2\omega^2} \qquad (3\text{-}9)$$

$\frac{b}{a}$ is the dynamic magnification.

In the Texas S-36 geophone a 15 KΩ damping resistance is built in, resulting in a 6KΩ external load. This according to the manual corresponds to h = 0.5 or $\lambda = 2\pi$. When h = 1 the damping is critical, and h = 0.5 corresponds to a damping ratio of 1:6. With these particular constants, calling the frequency f, equation (3-8) can be written:

$$\tan \delta = \frac{2f}{4-f^2}$$

With the Willmore Mark I seismometer a 1000Ω damping resistance was used. The average damping ratio was measured to be 1:3 1/2, corresponding to h = 0.369.

Using these constants the phase difference between the output of the two seismometers was calculated and the results are shown in graphical form in figure 4. An experimental test on this theoretical curve was made by recording 7 1/2 cps microseisms (at University campus, night-time) with a vertical Willmore on one trace and a Texas S-36 seismometer on another trace. The average of 15 readings was $4.3 \pm 1.2$ milliseconds corresponding to $11^{o}.6 \pm 3^{o}.2$, with the Willmore output lagging behind the Texas output as

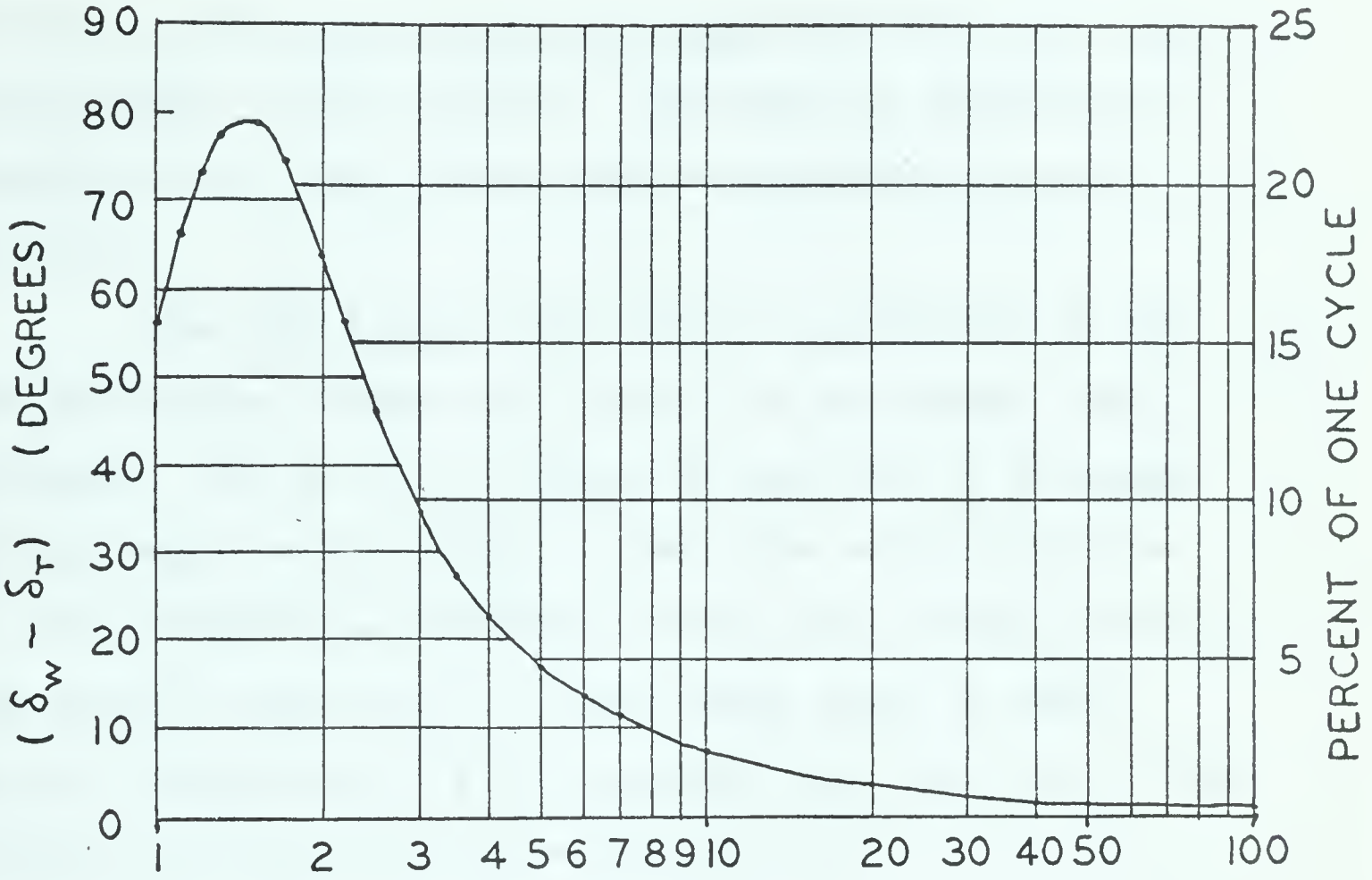


$\delta_W$ : Phase lag recorded by Willmore I seismometer ( 1 cps ).

$\delta_T$ : Phase lag recorded by Texas ( S-36) seismometer ( 2cps ).

FIG. 4.

predicted. The result is in good agreement with the theoretical result, which is $10^{o}.4$. As usual in geophysical literature the $\pm$ sign stands for the estimated standard deviation.

The next logical step after a comparison of the phase difference between two outputs is to compare their amplitudes. The e. m. f. induced in the coil of a seismometer is equal to a constant K times the velocity of the coil with respect to the magnet so with the harmonic motion given by (3-3) the e. m. f. is $Kb\omega$ (mean level to peak). When coil resistance is r and external load is R the voltage U across the outlets of the seismometer is

$$U = \frac{RKb\omega}{R+r} \qquad (3\text{-}10)$$

The dynamic magnification may be rewritten from (3-9)

$$\frac{b}{a} = \left[\left(1-\frac{fn^2}{f^2}\right)^2 + 4h^2\frac{fn^2}{f^2}\right]^{-1/2} \qquad (3\text{-}11)$$

fn is the natural frequency of the seismometer, it equals $\frac{n}{2\pi}$. The maximum speed of ground motion is called v (reached twice in a cycle); from (3-1)

$$v = a\omega = 2\pi fa \qquad (3\text{-}12)$$

Then, combining (3-10), (3-11) and (3-12):

$$U = K \cdot \frac{R}{R+r} \cdot \left[\left(1-\frac{fn^2}{f^2}\right)^2 + 4h^2\frac{fn^2}{f^2}\right]^{-1/2} \cdot v \qquad (3\text{-}13)$$

This formula is somewhat similar to the one given in the manual.

The system responds linearly to the voltage U, but the amplification depends on frequency, high cut filter setting and the attenuation setting used on the amplifier.

For the Texas S-36 seismometer the constant K is given in the manual to be 8.33 volts/inch/sec or 3.28 volts/cm/sec. The total external load for the Texas seismometer coil when used with the Very Low Frequency Refraction System is 6KΩ, the coil resistance is 4000Ω.

To determine the value of K for the Willmore seismometer a comparison of Willmore output with Texas output for 20 cps was made. First one sample of such microseisms (Physics Building, basement) was recorded with Texas seismometers on traces 1 and 2, then one recording was made with the Texas seismometer (No. 1023) replaced by Willmore Mark I (No. 84694), set up for vertical operation. By comparisons with the common seismometer on trace 2 it was possible to make the comparison independent of differences in amplification of the two amplifiers. The result was that K for the Willmore I seismometer is 0.955 volts/cm/sec. For high frequencies, i.e., when the dynamic magnification is 1, the ratio of the Willmore amplitude to the Texas amplitude with damping resistance used will hence be 0.313. For lower frequencies the difference between the frequency responses of the two instruments must be taken into account. The change of trace amplitude caused by this effect is shown on figure 5; the

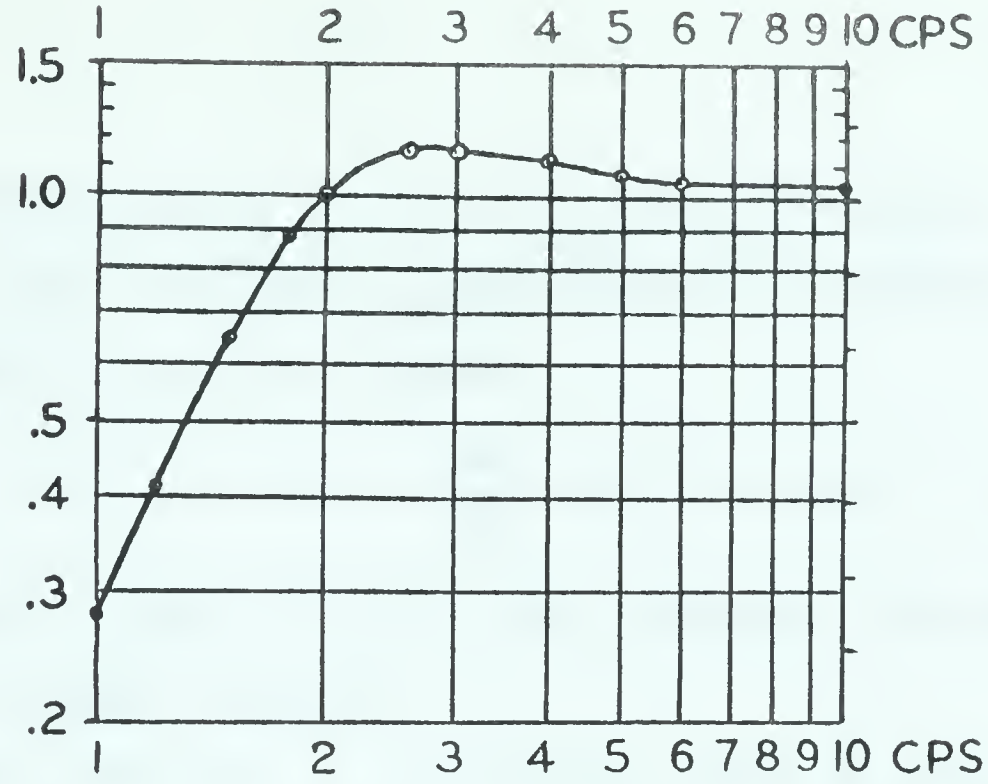


Normalized velocity sensitivity of Texas S-36 seismometer

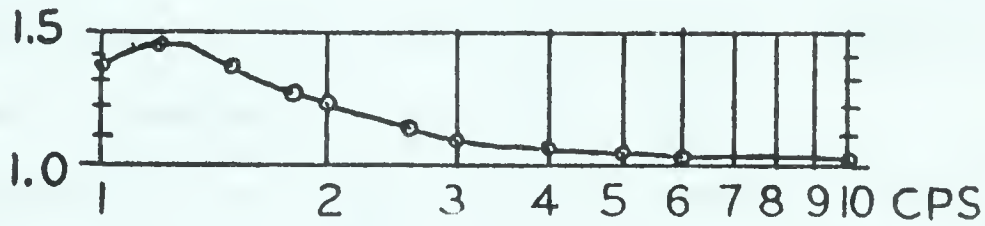


Normalized velocity sensitivity of Willmore I seismometer

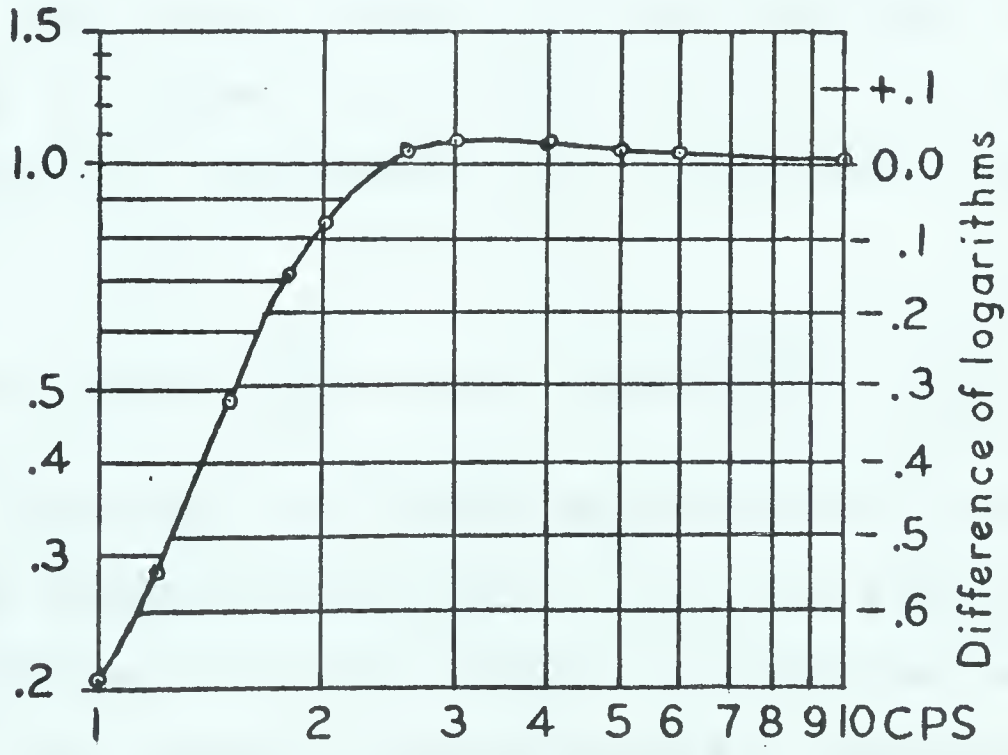


Normalized ratio $\frac{\text{Texas}}{\text{Willmore}}$ of velocity sensitivities

Normalized ɔ: Equals one at high frequencies

FIG. 5.

response is normalized to be one for high frequencies.

The input voltage to amplifiers can be derived from the trace amplitude by the formula:

$$\log U = \log A + \frac{a_T}{20} + \log B + \log C \qquad (3\text{-}14)$$

Where U - input to amplifiers in volts (measured from peak to average voltage)

A - trace amplitude in millimeters (peak to peak)

B - correction factor due to insertion of filters

C - a constant of the amplifier system, implicitly given in manual to be $2.95 \cdot 10^{-7}$

$a_T$ - attenuation setting, variable from 0 to 66 db of energy attenuation.

Table 1 shows log B as a function of filter settings and of the frequency; the values are derived from the filter response curve in the manual. Combining (3-11), (3-13) and (3-14) yields:

$$\log v = \log A + \frac{a_T}{20} + \log B + \log\left[\frac{C(R+r)}{KR} \cdot \frac{1}{b/a}\right] \qquad (3\text{-}15)$$

This formula shows that the dynamic magnification b/a is a measure of the velocity sensitivity. Since b/a equals one at high frequencies, it can be called the normalized velocity sensitivity. The values of this quantity are shown in graphical form in figure 5. Combining (3-12) and (3-15):

$$\log a = \log A + \frac{a_T}{20} + \log B + \log\left[\frac{C(R + r)}{KR \cdot 2\pi \cdot b/a}\right] - \log f \qquad (3\text{-}16)$$

The formula (3-15) for the ground velocity is somewhat simpler than (3-16) inasmuch as the frequency dependence only shows in the factor b/a as a low-cut filter effect and in the factor B as a high-cut filter effect; in between the response is flat. Thus it is easier to compare amplitudes connected with different frequencies when ground velocities are used, and also the smallest measurable seismic noise will have a flat frequency dependence in the range considered. The use of ground velocities to measure vibrations can also be considered as a compromise between the use of ground amplitude ($\propto$ ground velocity times $f^{-1}$) and ground accelerations ($\propto$ ground velocity times f).

Measuring a in Ångströms and v in Ångströms/sec, the numerical value of K will be modified so that the factor $\frac{C(R+r)}{KR}$ attains the values: 15.0 for the Texas seismometer and 4.70 for the Willmore seismometer.

The resulting values of the quantity $\log \frac{C(r+r)}{KR} \cdot \frac{1}{b/a}$ are shown in Table II for the Texas S-36 seismometer.

To get the ground velocity in Ångströms/sec, formula (3-15) is convenient to use with Tables 1 and 2. Ground amplitude if desired may then be obtained by (3-12) or (3-16).

The magnifications derived from the above formulas are only half of those obtained by means of Dr. Garland's curve (Weaver 1962). The reason is that in this work the use

of peak to peak amplitudes was preferred for the trace amplitudes, but not for the velocities of the ground motion.

TABLE I

Log B, the Reduction for the Attenuation due to Filters.

| Frequency CPS | HCF - FILTER SETTING | | | | | |
|---|---|---|---|---|---|---|
| | 8 | 12 | 16 | 24 | 32 | 48 |
| 2 | 0.26 | 0.22 | 0.17 | 0.10 | 0.05 | 0.00 |
| 3 | 0.28 | 0.22 | 0.17 | 0.10 | 0.05 | 0.00 |
| 4 | 0.31 | 0.23 | 0.17 | 0.10 | 0.05 | 0.00 |
| 5 | 0.36 | 0.25 | 0.17 | 0.10 | 0.05 | 0.00 |
| 6 | 0.41 | 0.28 | 0.17 | 0.10 | 0.05 | 0.00 |
| 7 | 0.47 | 0.31 | 0.19 | 0.11 | 0.05 | 0.00 |
| 8 | 0.53 | 0.35 | 0.21 | 0.12 | 0.06 | 0.00 |
| 9 | 0.57 | 0.38 | 0.23 | 0.13 | 0.06 | 0.00 |
| 10 | 0.66 | 0.42 | 0.25 | 0.14 | 0.06 | 0.01 |
| 12 | 0.78 | 0.49 | 0.30 | 0.16 | 0.07 | 0.01 |
| 14 | 0.92 | 0.58 | 0.36 | 0.19 | 0.08 | 0.02 |
| 16 | 1.06 | 0.66 | 0.41 | 0.22 | 0.10 | 0.04 |
| 18 | 1.19 | 0.74 | 0.46 | 0.26 | 0.12 | 0.05 |
| 20 | 1.31 | 0.82 | 0.52 | 0.29 | 0.14 | 0.06 |
| 22 | | 0.90 | 0.58 | 0.33 | 0.16 | 0.08 |
| 24 | | 0.98 | 0.63 | 0.37 | 0.19 | 0.09 |
| 26 | | 1.05 | 0.69 | 0.41 | 0.21 | 0.11 |
| 28 | | 1.12 | 0.74 | 0.45 | 0.24 | 0.13 |
| 30 | | 1.19 | 0.80 | 0.50 | 0.27 | 0.14 |
| 35 | | 1.37 | 0.95 | 0.59 | 0.33 | 0.19 |
| 40 | | 1.55 | 1.08 | 0.70 | 0.40 | 0.24 |
| 45 | | | 1.21 | 0.81 | 0.48 | 0.28 |
| 50 | | | | 0.90 | 0.55 | 0.34 |

TABLE II

Values of the Quantity $\log \frac{C(R+r)}{KR \cdot b/a}$ for the Texas S-36 Seismometer, to be used with Formula (3-15).

| Frequency | 1 | 1.5 | 2 | 2.5 | 3 | 4 | 5 | 6 | 7 |
|---|---|---|---|---|---|---|---|---|---|
| $\log \frac{C(R+r)}{KR \cdot b/a}$ | 1.74 | 1.37 | 1.18 | 1.12 | 1.12 | 1.14 | 1.15 | 1.16 | 1.16 |

| Frequency | 8 | 9 | 10 | 11 | 12 | 13 | 14 | >14 |
|---|---|---|---|---|---|---|---|---|
| $\log \frac{C(R+r)}{KR \cdot b/a}$ | 1.16 | 1.17 | 1.17 | 1.17 | 1.17 | 1.17 | 1.18 | 1.18 |

# IV. THREE TO TEN SECOND MICROSEISMS AT STATION EDMONTON JULY AND AUGUST 1963

## 4.1 Introduction

Most microseisms in the 3 to 10 second period range are caused by disturbed weather over large bodies of water. They show a clear seasonal variation resulting in larger mean periods and mean amplitudes in winter as compared to the summer. The distribution of amplitudes in a given month is markedly skew, making it possible to distinguish between microseismic storms and the usual background microseisms. The term "microseismic storm" is used to describe a period where the amplitudes are larger than normal.

Discussion on various general aspects of the 3 to 10 second microseisms was given in the introduction, and further discussions will follow in section 4.5a. The present chapter will chiefly be devoted to the interpretation of microseisms recorded at station Edmonton (the University of Alberta seismic observatory).

## 4.2 Amplitudes and Periods

For the two months, July and August 1963, the amplitudes of 3 - 6 second microseisms at station Edmonton

on the LPZ (i.e. long period vertical seismograph) were measured at 6 hour intervals. Each amplitude was the average of maximum amplitudes in ten minute intervals. The results are given in figure 6. Most of the periods were between 4 and 5 seconds and therefore it was found reasonably accurate to use a common factor to convert peak to peak trace amplitude to center to peak ground amplitude. The factor used corresponded to the period of 4 1/2 seconds.

It will be seen from figure 6 that it is easy to locate microseismic storms; the most conspicious ones occurred at July 6 and at August 13, 15 and 28.

Only on two occasions did periods longer than 6 seconds occur with an amplitude exceeding that of the simultaneous 3 - 6 second microseisms. One occasion was August 6 with a few beats of 8 second microseisms having an amplitude of 0.14 microns. The other occasion was a microseismic storm of 8 second microseisms. This storm was noticable from August 23, $9^h$ GMT to August 26, $1^h$ GMT. The amplitude was gradually increasing through the value 0.21 microns at August 24, $6^h$ GMT to 0.35 microns at August 24, $18^h$ GMT. These 8 second microseisms are not shown in figure 6.

The period of the dominant microseisms, i.e. of the microseisms that produced well developed maxima on Z, were measured whenever a direction of approach was determined

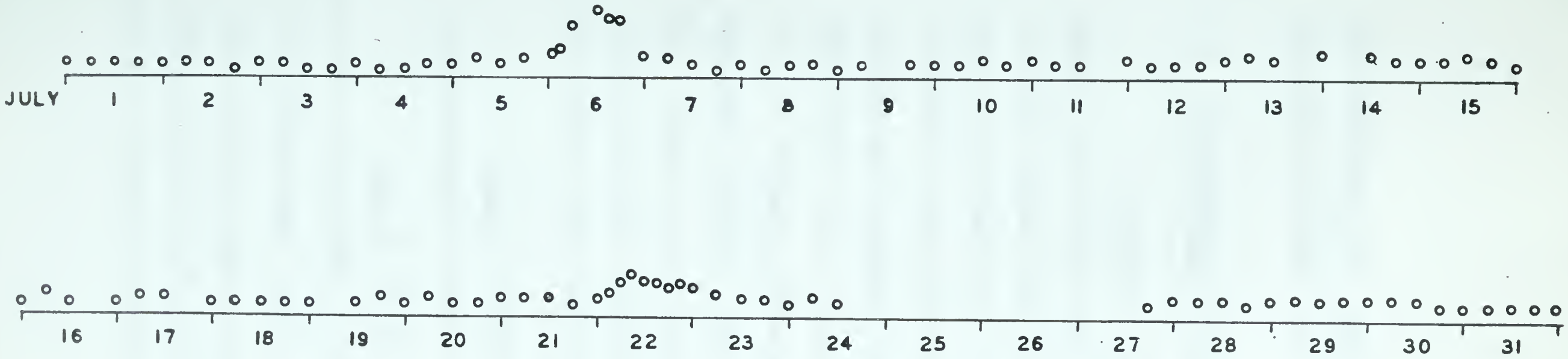


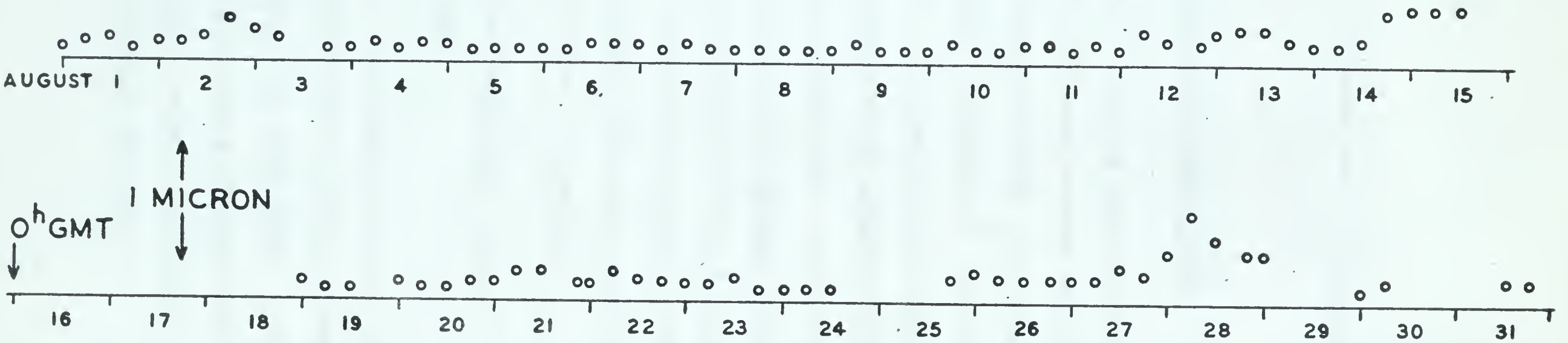


FIG. 6. Amplitudes of 3-6 second microseisms on the longperiod vertical ( LPZ ) recorded at station Edmonton, the University of Alberta seismic observatory, during July-August 1963.

(see section 4.4). The results of these period measurements are shown in Table III.

## 4.3 The Weather Situation in July and August 1963

A complete description of what is known about the weather situation along the North American coasts during July and August 1963 would take several books. It is available on punched cards. Some general features of the weather situation associated with periods of anomalous activity of microseisms, however, could be extracted by looking through the weather maps. These maps were kindly made available to me by E. Reinelt, Meteorological Service of Canada, Edmonton Municipal Airport. The information given in this section will be used in the discussions in section 4.5. The winds quoted are winds reported from weather stations, generally the highest wind reported from the area in question.

July 5, $6^h$ GMT. A 998 mb barometric low is situated near Pt. Barrow moving ENE.

July 6, $6^h$ GMT. The low has deepened to 996 mb, and is now at 75°N, 121°W (McClure Strait). For the season it is quite deep, and it is producing 30 knot winds. The other coastal areas are fairly quiet during this period. Winds: 0-5 knots at the Californian, Oregon, Washington and B.C. coasts; 15 knots at the Alaskan SW coast.

July 6, 18$^{h}$ GMT. The low has moved to 77°N, 120°W.

July 7, 6$^{h}$ GMT. The low has deepened to 992 mb and is now situated at 79°N, 110°W.

July 8, 0$^{h}$ GMT. The low has weakened to 1000 mb and moved to 79°, 120°W.

July 13, 6$^{h}$ GMT. A 996 mb low in the Hudson Bay is producing 20 knot winds.

July 21, 18$^{h}$ GMT. A 1004 mb low is situated at 48°N, 132°W, 4 degrees off the coast of B. C.

July 22, 0$^{h}$ GMT. The low is just one degree off the coast and has deepened to 1000 mb and is producing 30 knot winds. Maximum wind observed in Hudson Bay, The Canadian Arctic and Labrador is 15 knots.

July 22, 12$^{h}$ GMT. The low has moved north along the coast to 53°N and has deepened to 996 mb. The maximum wind along northern and eastern Canadian coasts is still 15 knots.

July 23, 0$^{h}$ GMT. The low has filled up, but 30 knot winds still occur.

July 23, 6$^{h}$ GMT. 20 knot winds occur at the Pacific coast and in the Hudson Bay.

August 13, $6^h$ GMT. A low in the northern part of Labrador is associated with 25 knot winds. Along the coast of B. C. 20-40 knot winds occur.

August 13, $18^h$ GMT. A frontal system now developed in the Hudson Bay area and a low at the B. C. coast are both producing 20 knot winds.

August 14, $12^h$ GMT. A 1012 mb low at 68°N, 110°W (Coronation Gulf) producing 15 knot winds.

August 14, $18^h$ GMT. The low has moved to 68°N, 106°W and winds have increased to 25 knots. The winds along the B. C. coast and over Hudson Bay are calm or fairly light.

August 15, $6^h$ GMT. The low is 1008 mb at 72°N, 95°W with 25 knot winds. Another low is situated at the northern part of Labrador.

August 15, $18^h$ GMT. The Labrador low is now producing 30 knot winds.

August 22, $0^h$ GMT. Two deep lows (both 996 mb, fairly deep for a summer low) are associated with 25-30 knot winds. One is at 48°N, 166°W (the Pacific, 5 degrees from the Aleutian Islands) slowly moving east, while the other is at 58°N, 165°W (the Bering Sea) rapidly moving towards the Bering Strait.

August 22, 12$^{h}$ GMT. The lows have deepened to 992 mb at 47°N, 162°W and 984 mb at 62°N, 167°W.

August 23, 0$^{h}$ GMT. The cyclones are still very active; the Pacific one is 1000 mb at 50°N, 160°W with strong winds (35 knots) in an annular pattern 3-5 degrees from the center of the cyclone. The other low is now 984 mb at 69°N, 167°W (north of the Bering Strait) and is producing 30 knot winds.

August 23, 18$^{h}$ GMT. The Pacific low is now 1004 mb and at 53°N, 157°W with fronts extending 10 degrees S and SE of that point and with 25 knot winds at these fronts.

August 24, 12$^{h}$ GMT. The low has been filled up, but 20 knot winds still occur in the Pacific.

August 28, 0$^{h}$ GMT. A low in Baffin Bay produces 25 knot winds in Greenland. The Canadian Arctic is also disturbed with 25 knot winds at Coronation Gulf.

August 28, 6$^{h}$ GMT. The Baffin Bay low produces 25 knot winds in Greenland, a front system in the Canadian Arctic produces 25 knot winds at 120°W.

August 28, 12$^{h}$ GMT. The low in Baffins Bay produces 25 knot winds in the straits north of Hudson Bay. The Arctic front system produces 20 knot winds at Coronation Gulf.

## 4.4 The Directions of Approach

The directions of approach were determined in 26 cases selected from the months July and August 1963 at station Edmonton. The method used was Jensen's method, described in section 2.5. Altogether 1258 slopes were read.

The results are shown in Table III, and some of the NE diagrams used during the determinations are shown in Figure 7. T is the period as measured during the time interval used for the determination of the direction of approach; $\alpha$ is the direction of approach, i.e. the directions that the waves come from, measured from north, positive towards east. The reliability measure p and the "Rayleigh amplitude" $A_R$ are defined in section 2.5. The significance of the three different categories, A, B, and C is given below; n is the number of points.

At first 11 determinations were made in order to find the directions of approach of the microseismic storms. Two or three determinations were made on each storm, and the results agreed, so that the directions determined for a given storm always belonged to the same or to two adjacent octants. The 12 determinations of the approach of storm microseisms are labeled "category A".

The weather maps were studied, and the correlation with wind storms in the Arctic, in Hudson Bay and at Labrador

TABLE III

The Directions of Approach of Microseisms at Edmonton Determined by Jensen's Method.

| DATE | Time Interval used h | m | T (sec) | p | α | category | n | $A_R$ (milli-microns) | Octant |
|---|---|---|---|---|---|---|---|---|---|
| July 2 | 10 | 01-05 | 4.3 | 4 | +159° | C | 20 | 18 | S |
| 6 | 5 | 02-08 | 5.1 | 10 | + 12° | A | 19 | 288 | N |
| | 8 | 53-56 | 5.1 | 9 | + 12° | A | 21 | 244 | N |
| | 18 | 01-07 | 4.8 | 9 | + 31° | A | 20 | 172 | NE |
| 7 | 6 | 01-08 | 5.2 | 10 | + 54° | B | 23 | 91 | NE |
| 10 | 10 | 01-06 | 3.9 | 4 | 0° | C | 26 | 14 | N |
| 12 | 10 | 01-05 | 4.1 | 3 | +110° | C | 25 | 20 | E |
| 13 | 6 | 01-06 | 4.0 | 5 | +108° | B | 35 | 26 | E |
| | 6 | 06-10 | 3.9 | 1 | +148° | B | 26 | 18 | SE |
| 19 | 10 | 01-06 | 4.1 | 1 | -166° | C | 29 | 7 | S |
| 22 | 9 | 01-04 | 4.0 | 2 | + 44° | A | 24 | 30 | NE |
| | 11 | 56-63 | 4.4 | 0 | + 90° | A | 24 | 37 | E |
| 23 | 10 | 01-05 | 4.0 | 5 | + 63° | C | 30 | 33 | NE |
| 24 | 10 | 01-06 | 3.5 | 4 | + 37° | C | 27 | 22 | NE |
| 29 | 10 | 01-07 | 4.1 | 3 | + 56° | C | 24 | 14 | NE |
| Aug. 3 | 10 | 01-06 | 4.6 | 1 | + 97° | C | 28 | 7 | E |
| 4 | 10 | 01-07 | 4.2 | 5 | + 78° | C | 26 | 14 | E |
| 10 | 10 | 01-07 | 3.8 | 3 | + 42° | C | 33 | 11 | NE |
| 13 | 6 | 01-03 | 4.4 | 7 | + 68° | A | 19 | 95 | E |
| | 9 | 01-03 | 4.5 | 7 | +105° | A | 18 | 128 | E |
| | 12 | 01-04 | 4.4 | 10 | + 50° | A | 19 | 108 | NE |
| 14 | 17 | 57-63 | 4.5 | 3 | + 72° | B | 18 | 82 | E |
| 24 | 5 | 55-61 | 8.2 | 9 | - 71° | A | 24 | 209 | W |
| | 6 | 27-28 | | | | | | | |
| | 16 | 53-59 | 7.9 | 9 | - 79° | A | 27 | 164 | W |
| 28 | 3 | 01-04 | 5.2 | 7 | + 51° | A | 22 | 264 | NE |
| | 12 | 01-04 | 5.8 | 1 | - 15° | A | 20 | 74 | N |

Times are given in GMT.

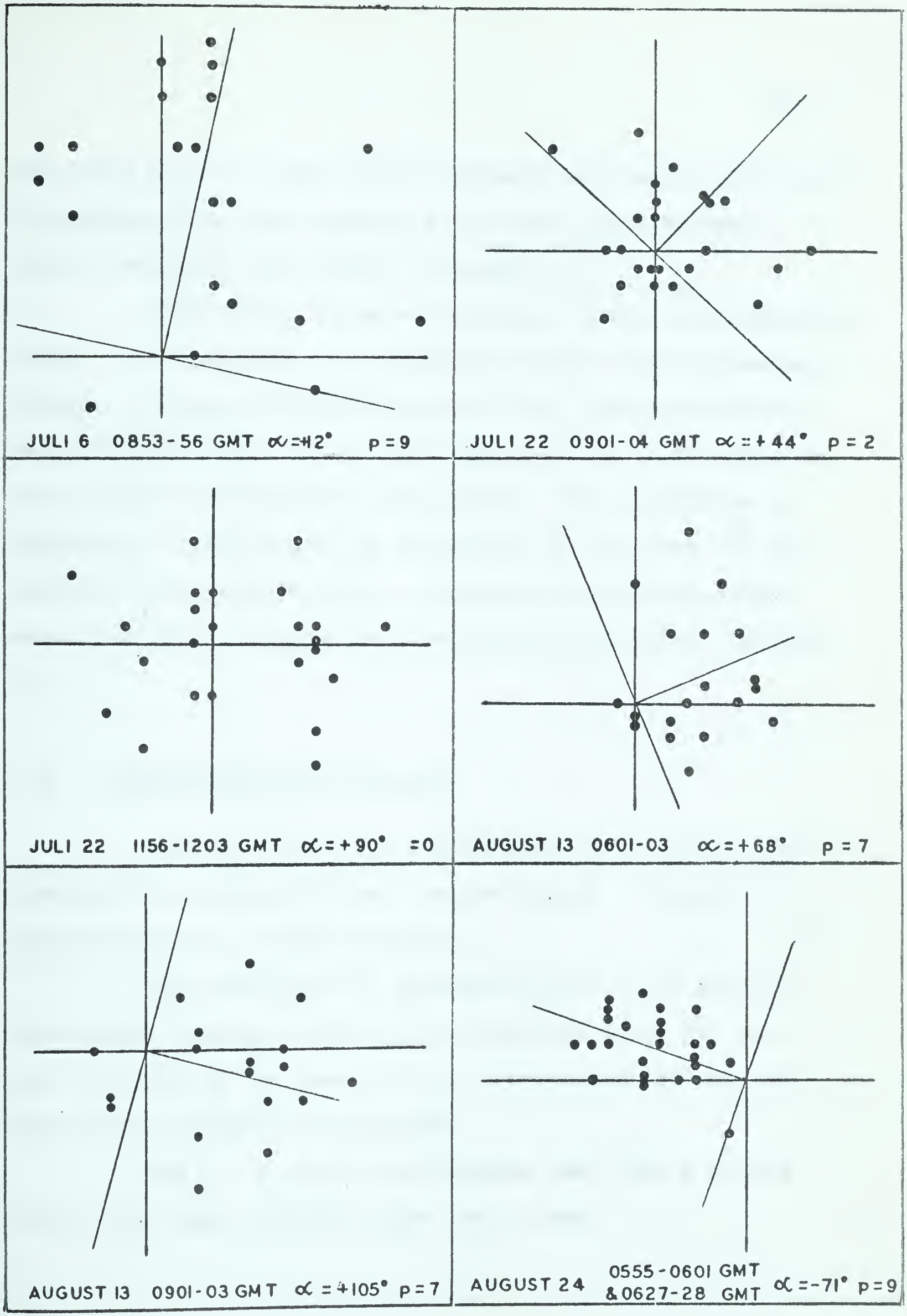


FIG. 7. NE-diagrams, used to get some of the directions listed in table III.

was found to be so good that an attempt to predict directions of approach from some weather situations was undertaken. These directions are labeled "category B".

Finally ten dates were selected among the remaining dates, i.e. among the quiet periods between the microseismic storms. A table of random numbers (Hald, 1951) was used to select these dates. The record amplitude at these dates was only a small fraction of a millimeter. The directions of approach at these dates was determined at the time $10^h$ GMT, where the long period noise, presumably of thermal origin, was a low level. These ten directions are labeled "category C".

4.4a Distribution into Octants

Table IV shows the distribution into octants for observations having different period ranges. Category C observations are listed separately.

The directions of approach of the 3 - 5 second microseisms scatter chiefly in the octants E and NE, and this tendency is the same for the microseismic storms and for the low activity microseisms.

The 5 - 6 second microseisms came from N and NE and all the data originate from two storms.

TABLE IV

Joint Distribution Period T in seconds versus the Octant of the Direction of Approach.

| | CATEGORY C | CATEGORY A and B | | | | |
|---|---|---|---|---|---|---|
| | 3<T<5 | 3<T<5 | 5<T<6 | 6<T<7 | 7<T<9 | TOTAL |
| N | 1 | 0 | 3 | 0 | 0 | 4 |
| NE | 4 | 3 | 2 | 0 | 0 | 9 |
| E | 3 | 5 | 0 | 0 | 0 | 8 |
| SE | 0 | 1 | 0 | 0 | 0 | 1 |
| S | 2 | 0 | 0 | 0 | 0 | 2 |
| SW | 0 | 0 | 0 | 0 | 0 | 0 |
| W | 0 | 0 | 0 | 0 | 2 | 2 |
| NW | 0 | 0 | 0 | 0 | 0 | 0 |
| TOTAL | 10 | 9 | 5 | 0 | 2 | 26 |

No 6 - 7 second microseisms were observed during the two months under study.

The 7 - 9 second microseisms were observed with sufficient amplitude only during one 8 second microseismic storm. The reliability of these directions is very good (p = 9 in both determinations) and they are the only observations in the western octant.

## 4.5 Interpretation of the Directions of Approach

During the interpretation, some quantitative work was done based on Longuet-Higgins' theory; however only in cases where this theory is mentioned does the conclusion depend on this theory; conclusions concerning distributions of directions of approach and selective barriers are independent of assumptions concerning the mechanism of the generation of microseisms.

### 4.5a Microseisms Expected from Given Wind Velocities According to Longuet-Higgins' Theory

If Longuet-Higgins' theory is used as a working hypothesis, generation of 3-8 second microseisms will only be expected from large bodies of open water, and this consequence agrees with the observations.

Longuet-Higgins' theory was further developed by

Hasselmann (1963), who took the areal extent of the source into account. He also pointed out that microseisms would be produced, not by interaction between gravity waves having exactly equal and opposite wave numbers, but rather by interactions between waves with slightly different wave numbers, that produce compressional waves of finite horizontal phase velocity in resonance with a trapped mode of the waveguide.

The theory predicts proportionality between the amplitude of microseisms and the square of the waveheights of the interfering waves. This prediction was confirmed by Hjortenberg (1963). The square can be taken to be proportional to the energy of the waves, and this energy, according to Defant (1961, p. 55) is, for a fully arisen sea, proportional to the fifth power of the wind velocity.

The periods of wind waves to expect from a given wind velocity of long duration and large horizontal extent was given implicitly by Defant (1961, p. 54):

$$T_{max} = 0.40\ v \qquad (4\text{-}1)$$

where $T_{max}$ is the water-wave period associated with the peak of the power spectrum and v is the wind speed in knots.

Hence 20 and 30 knot winds would produce water wave spectra with peaks at 8 and 12 seconds, and from

Longuèt-Higgins' theory 4 and 6 second period microseisms would be expected. (Longuet-Higgins, 1950).

This prediction agrees with the microseismic storms investigated in Edmonton. The periods associated with category A observations of non-Pacific origin were 4.0 - 5.8 seconds and the winds observed in the suspected source areas were 20 - 30 knots.

4.5b Comparison of Microseisms with High Winds in the Pacific

Three cases of disturbed weather in the Pacific are described in section 4.3. The first case was between July 22, $0^h$ GMT and July 23, $0^h$ GMT. Winds were 30 knots, while winds elsewhere were less than 15 knots; it should be mentioned, however, that the weather maps available did not permit investigation of the weather along the eastern coast of U. S. A. The directions of approach determined are in the octants E and NE, but the p's are very small and figure 7 shows that the points are scattered in all directions. The $A_R$ is only one third of the $A_R$ determined on August 13, at which time the vertical amplitude was similar. This could indicate that microseisms of Pacific origin account for roughly one-third of the amplitude. From the weather situation, however, the Pacific microseisms

could be expected to exceed other microseisms. From Longuet-Higgins' theory they could be expected to have at least $2^5 = 32$ times the amplitude from other sources, but their amplitude was smaller, and this is interpreted as a very heavy damping of Pacific microseisms.

The second case is August 13, $6^h$ GMT. This was a storm affecting local areas of the Pacific coast and was not associated with any extended low pressure system. It appears from figure 7 that no perturbation of the microseisms were produced.

The third case at August 22 to August 23 was an extended low pressure system in the Pacific. It will be discussed in the next subsection.

### 4.5c Eight Second Microseisms

Only one microseismic storm of 8 second period occurred during the two months investigated. The amplitudes are described in section 4.2. From August 24, $6^h$ GMT to August 24, $18^h$ GMT, these microseisms dominated over shorter period microseisms, and the directions of approach could be determined. The amplitude was steadily increasing until August 24, $18^h$ GMT. For the next 24 hours no record was available and after that the amplitudes were again very small.

Both directions of approach were characterized by p = 9 and they were pointing towards the B. C. - Alaska boundary at the Pacific coast.

The weather situation in the Pacific had no unusual features during the time of the 8-second microseismic storm, so the weather during this period could not explain it.

Now let us apply Longuet-Higgins' theory as a working hypothesis:

Since no low pressure with a simultaneous generation of water waves with different directions is available, it is reasonable to attribute the microseisms to interference between in-coming and reflected swells with a period of 16 seconds.

For most of the path the water is deeper than half a wavelength and the amplitude is small compared to the wavelength, hence from the work of Barber and Tucker (1962):

$$V_{group} = \frac{gT}{4\pi} \qquad (4\text{-}2)$$

Thus the group velocity of a 16 second gravity wave is 0.405 degrees per hour.

According to Defant (1961, p. 53) the power density of the water wave energy at a period of 16 seconds can be expected to be 8 1/2 times the power density when the wind velocity is 40 knots as compared to the power density when

the winds have a speed of 30 knots. During August 22, $6^h$ - $18^h$ GMT, the strongest winds reported were 30 knots, but at August 23, $0^h$ GMT the maximum of all the winds reported from the low occurred. This wind speed was 35 knots, and an annular pattern of equidistant isobars made it reasonable to assume that 35 knot winds occurred throughout this annular pattern, 3 - 5 degrees from the center.

The distance from the northernmost point of the B. C. Coast to the closest point of this annular pattern is 12 degrees. This corresponds to 30 hours of travel time for the 16 second water waves, so these waves would arrive at August 24, $6^h$ GMT.

The distance at which the largest amount of wind energy in the annular zone has a direction towards the continent will correspond to the distance to the center of the low. This distance is 17 degrees, and hence these large amplitude waves are expected to arrive 42 hours later, i.e. at August 24, $18^h$ GMT.

Now the interval between August 24, $6^h$ GMT and August 24, $18^h$ GMT is exactly the interval where the microseism amplitude is steadily increasing to the high level at Edmonton.

Furthermore, 35 knot winds would according to (4-1) produce water waves with a power density peak at 14 seconds, and according to Defant (1961, p. 53) the range between the half power points is approximately one octave, so the 16 second water waves are well within the period range expected.

The consequences from the use of Longuet-Higgins' theory as a working hypothesis are thus in good agreement with these observations.

A swell having a period of 8 seconds from the same source cannot account for the observations, because it travels at half the speed and would arrive at least 30 hours late. It is also impossible that the same low could have generated the 8 second water waves at an earlier time, because the low was moving toward the continent with a speed approximately equal to the group velocity of 8 second gravity waves.

Since wavegauge recordings were not available, it is impossible to prove that the period of the swell was 16 seconds and it can only be stated that such a swell is to be expected from the weather situation.

One additional feature of the 8 second storm may be worthwhile to point out: The azimuth at station Edmonton of the position of the Pacific low at August 23, $0^h$ GMT was $\alpha = -73^\circ$. This value agrees with the directions of approach of 8 second microseisms at station Edmonton 30 to 41 hours later.

This agreement can be explained by the action of swell at the coast using the modification of Longuet-Higgins' theory, introduced by Hasselmann (1963) and described in section 4.5a, and one additional assumption.

The argument is this: The wavefronts are perpendicular to the direction of wave propagation, and waves reflected from the coast may be assumed to have the most constructive interference with the incoming waves, when the direction of propagation of the reflected waves differs exactly 180° from the direction of the incoming waves. This assumption seems reasonable because then the particle motion is in phase along the crest; however, it is nothing but an assumption.

When such a 180° difference occurs, all the vectorial wavenumbers will lie on a straight line towards the course, and so will the differences between wavenumbers of incoming and reflected waves. The distribution of the absolute values of wavenumbers of incoming and reflected waves can be expected to be identical, and thus the differences between the vectorial wavenumbers will have a symmetrical distribution on the line towards the source of the swell. A certain range of these vectorial wavenumbers will satisfy the condition to set up seismic waves, and hence the seismic energy will be sent out in two directions; towards the source of the swell and away from this source.

The mechanism described here can explain the direction observed in Edmonton, and also the high accuracy of the determination; such an accuracy would result from a narrow sector of approach.

A fair proportion of the rocky shores of the islands in the suspected source area for the microseisms, have a direction perpendicular to the direction to the source of the postulated swell.

For this eight second storm, Longuet-Higgins' theory has explained the following: The period, the variation of the amplitudes with time, the direction of approach and the variability of the same.

The evidence given here favors Longuet-Higgin's theory of microseism generation for this particular storm.

### 4.5d Comparison Between the Directions of Approach and the Non-Pacific Storms.

The Arctic low of July 6 was moving along the western edge of the Arctic archipelago. The direction to the center of the low varied between $\alpha = -5^{o}$ and $\alpha = -1^{o}$, but the directions of approach of microseisms in Edmonton varied between $+12^{o}$ and $+ 31^{o}$.

This difference may be explained by the distribution of the polar ice. In most of the ~~open~~ Arctic Ocean the water is covered with ice all summer, and the winds would not produce microseisms. Between the islands of the archipelago the water is open in summer, and the bodies of water are large enough for the generation of microseisms.

At July 7, $6^h$ GMT, the low was deepening, but the microseismic storm had a small and decreasing amplitude. This may be due to the position of the low at 79°N; at such high latitudes most bodies of water are covered with ice, even in summer.

The deviation of the directions determined for July 13 is not unreasonable, considering the p's. Some of the microseisms could have their origin on the eastern coast of U. S. A. The direction to the southern edge of Hudson Bay is $\alpha = +81^o$.

The directions on August 13, $6^h$ GMT and $12^h$ GMT agrees well with $\alpha = 60^o$, which is the azimuth of the Hudson Bay low and the Labrador low. At $9^h$ GMT the source seems to be further south. The determination on August 14 deviates 70°, but for p = 3 such an error may occur.

The directions on August 28 agree well with the disturbed weather in Greenland and in the Canadian Arctic.

4.5e <u>The Distribution of the Directions of Approach. A Selective Microseismic Barrier in Western Canada.</u>

A significant tendency for the 3 - 6 second microseisms to arrive from the octants N, NE, and E was demonstrated in section 4.4a.

This feature may be explained by assuming a

barrier for such a microseisms between the Pacific and Edmonton. None of the directions of approach determined for microseisms with periods between 3 and 6 seconds fell into the sector between $\alpha = -71^{o}$ and $\alpha = -136^{o}$, in which the distance to the Pacific is shorter than to Hudson Bay. Since all the observations with periods between 5 and 6 seconds originate from only two storms, the conclusion of a microseismic barrier in western Canada has been restricted to the 3-5 second microseisms, but it is possible that the relative rareness of 5 - 6 second microseisms is caused by the same effect.

A large attenuation of 3 - 5 second microseisms of Pacific origin also agree with the discussion in section 4.5b, and in section 4.5c it is shown that an 8 second microseismic storm of Pacific origin was recorded, hence the barrier in western Canada can be described as selective.

The interval of azimuths pointing towards the Rocky Mountain system is from $\alpha = +145^{o}$ to $\alpha = -26^{o}$. This $189^{o}$ interval contains 2 out of the 24 determinations with 3 - 6 second periods. One of these directions was from July 2. Its deviation from the margin $\alpha = +145^{o}$ was less than the probable error. The other direction was from July 19; it had $p = 1$ and the smallest $A_R$ determined, hence its reliability is extremely low. Omission of two points could change its direction to north.

Thus the observations are consistent with the microseismic barrier along the Rocky Mountains, but this barrier could be anywhere between Edmonton and the Pacific coast.

The velocity of surface waves with periods 3 - 8 seconds have been investigated by many authors; examples are Gutenberg (1955), Lehmann and Ewing (1960) and Oliver (1962). Velocities were generally between 2 and 3.5 km/sec. Thus wavelengths for 4 second microseisms could be 8 km, while they could be 30 km for 8 second microseisms.

The selective microseismic barrier found could be explained if the severe lithological anomalies in Western Canada penetrate to the depth comparable to 8 km, but not to 30 km. Conclusions of this kind must be delayed, however, until the nature of the continental waveguides is settled, but it can be stated, that a final model of the crustal structure of Western Canada must be able to explain this selective barrier, unless surface topography can account for it.

This study is the first to demonstrate a barrier effect in Western Canada, but similar conclusions have been obtained in U. S. A. as shown by the following quotation from Oliver and Ewing (1958b):

"Carder found that all but two stations in the United States recorded microseisms of 4 to 7 seconds from a storm off the east coast. The exceptions were Berkeley

and Ukiah. Carder attributed this anomaly to the effect of either Sierra Nevada or the Central Valley of California ..... Carder also found a suggestion of better microseismic transmission across the eastern low lands than across the Rocky Mountain system."

The fact that no 5 - 9 second microseisms were found to arrive from the east is considered an effect of the summer season, where generation of such microseisms is less prominent than in winter. The continental path between Edmonton and the east coast is expected to transmit such microseisms efficiently; at least the 8 - 9 second periods, since Donn (1954) found Pacific microseisms with such periods at the Palisades with good directional characteristics.

## 4.5f Validity of the Basic Assumptions

The basic assumptions of Jensen's method are stated in section 2.5.

The first assumption requires that the particle motion of the Rayleigh-type waves is retrograde. No authors have reported prograde particle motion for periods longer than 3 seconds, and the discussion in section 1.2 shows that even $M_2$ waves can be expected to have retrograde particle motion for periods longer than 3 seconds. The same discussion, however, would make it reasonable to expect

prograde $M_2$-waves if the pertinent crustal model has an unusual low rigidity.

Since station Edmonton is located on unconsolidated shales, on a thick sedimentary cover, it may appear necessary to check if the particle motion at Edmonton for surface waves with periods longer than 3 seconds is retrograde.

Such a check is provided by the agreement between the observations, and the cases of disturbed weather in Hudson Bay, the Arctic and in the Pacific as described in sections 4.5c and 4.5d. In particular the observations from July 6 with p = 9 and p = 10 occurred with disturbed weather in the Arctic and quiet conditions at the Californian coast, so that the source of these microseisms can be considered well established.

No research was conducted specifically to test the validity of the second basic assumption, but the good agreement between observations with the large p value and the weather situation favors the adoption of this assumption.

## Conclusions

As a result of the discussions in this chapter it can be concluded:

1. A microseismic barrier in western Canada attenuated the 3 - 5 second microseisms of Pacific origin, so that

it was never observed to dominate over the other microseisms, but a storm of 8 second microseisms of Pacific origin was demonstrated.

2. The meteorological conditions associated with the 8 second microseismic storm favors the conclusion that it is caused by the interference of incoming and reflected swell at the Pacific coast in agreement with Longuet-Higgins' theory.
3. The period range observed for microseismic storms of non-Pacific origin agrees with the range predicted from the wind velocities using equation (4-1) and Longuet-Higgins' theory.
4. The 5 - 6 second microseisms observed at Edmonton during July and August occurred in two storms and originated in Arctic waters.
5. The most frequent approach for 3 - 5 second microseisms was NE and E.
6. Good correlation was found between the directions of approach determined for microseismic storms, and the directions expected from the disturbed weather at sea.

# V. STUDY OF THREE CYCLES PER SECOND MICROSEISMS

## 5.1 Introduction

While 2 cps microseisms are found quite persistently in many areas of the United States (Wilson, Vesiac Staff, 1962) a similar spectral peak has not been found in Alberta. During the 1962 field season no 2 cps wavelets were seen on the field records, but on the University of Alberta Observatory short period records it does show up occasionally (visual observation). Frequencies around 3 cps, however, show up quite consistently (but not everywhere at all times), and it is concluded that in Alberta the peak of the power spectrum tends to be at 3 cps rather than 2 cps.

In analogy with chapter IV the first sections of this chapter will present the experimental data obtained at University of Alberta, while the comparison with work done elsewhere, the interpretation and the final conclusions will follow in later sections.

While the field records showed that some locations in general had a much larger 3 cps amplitude than other locations, the following section describes a study showing that at one given location the average amplitude is much larger at some times than at other times.

## 5.2 Comparison Between Observatory Records and Local Wind

On the short-period observatory records many individual bursts of energy of a few minutes duration are present, some of them having a very regular appearance like 3 cps sinusoidal waves. Between these bursts some rather irregular background microseisms are always present and have a high content of the 3 cps frequency, though the 2 cps frequency is also present. A glance at a few records reveals a daily variation (indicating more quiet conditions at night), and this was originally thought mainly to be due to wind.

Figure 8(a) illustrates this relationship by comparing the background noise with the wind that was simultaneously observed at the International Airport. The amplitudes of the background noise were measured by ignoring the discrete periods of high activity, caused by traffic and farm machinery. The amplitudes were measured during the period June 12 - 30, 1963. Surprisingly, no clear correlation between background microseisms and wind is visible. To investigate whether this lack of correlation could be due to variation of wind from one location to another, figure 8(b) was made. The University of Alberta Observatory is 12 miles from the International Airport and the Municipal Airport is 17 miles from the International Airport. A clear correlation

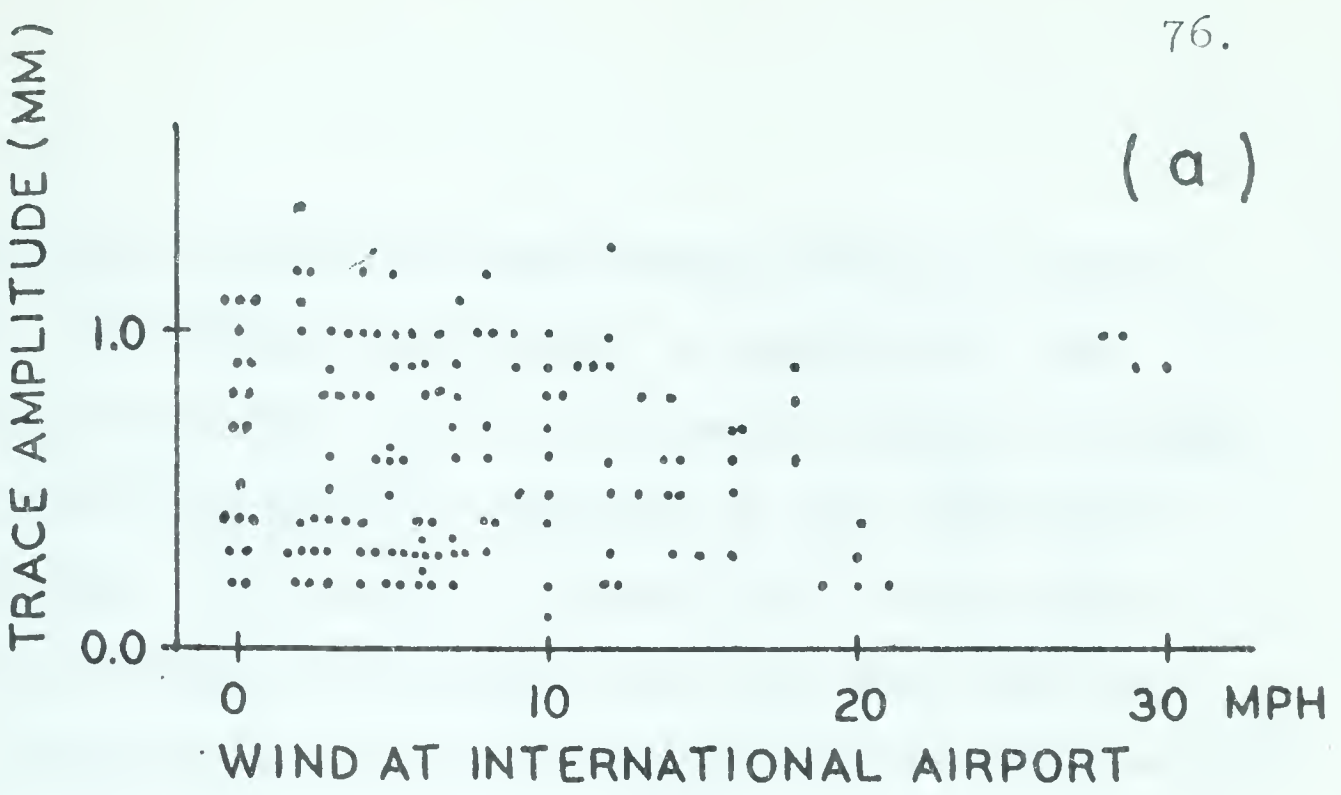


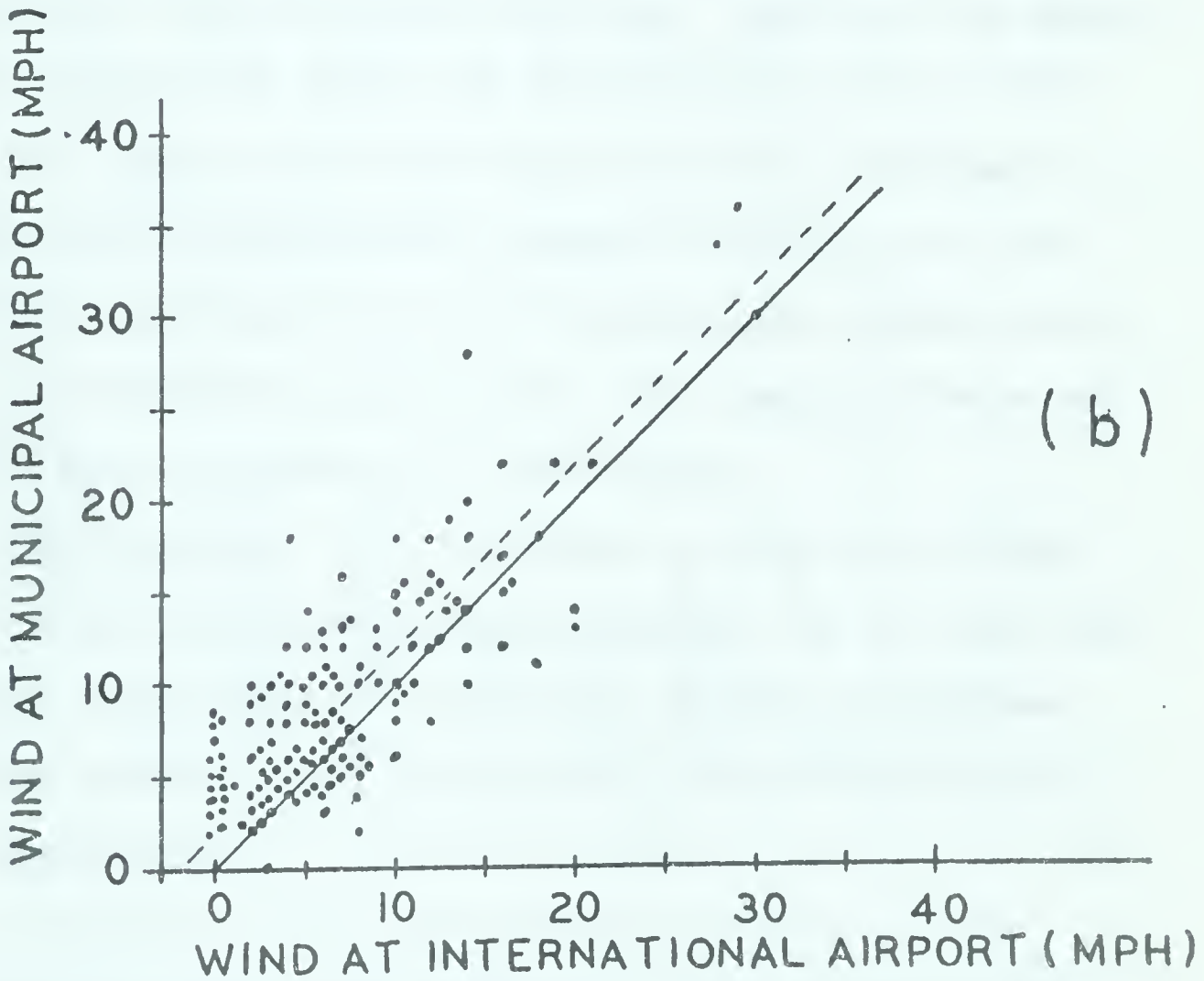


FIG. 8. June 12-30 1963, one dot per simultaneous 3-hourly observation of:

(a) U. of A. observatory SPZ 3 cps background noise versus wind velocity at International Airport.

(b) Wind velocity at Municipal Airport versus wind velocity at International Airport.

is demonstrated between the simultaneous winds at the two airports, and although the scatter is appreciable, the correlation is so good that it is possible, based on figure 8(b), to make a reasonable correction to the instruments that were used: The points in figure 8(b) do not group symmetrically about the identity line (the full line on figure), as they would if the frequency of occurrence of any given wind velocity were similar at the two places and if the instruments were reading correctly. However, the distribution is symmetrical about the dashed line, which is the identity line that would have resulted if the instruments at the Municipal Airport were reading as little as 1 mph more and the instruments at the International Airport were reading 1 mph less than true wind. Such small differences may be difficult to detect by other means.

Now assume: 1. Differences in wind velocities between the Edmonton International Airport and the Municipal Airport are comparable to differences in wind velocities between the International Airport and the University of Alberta Observatory.

2. Wind is the major source of the 2 - 3 cps background noise at the University of Alberta Observatory.

Then the spread observed in figure 8(b) is too small to make the expected correlation between wind at the

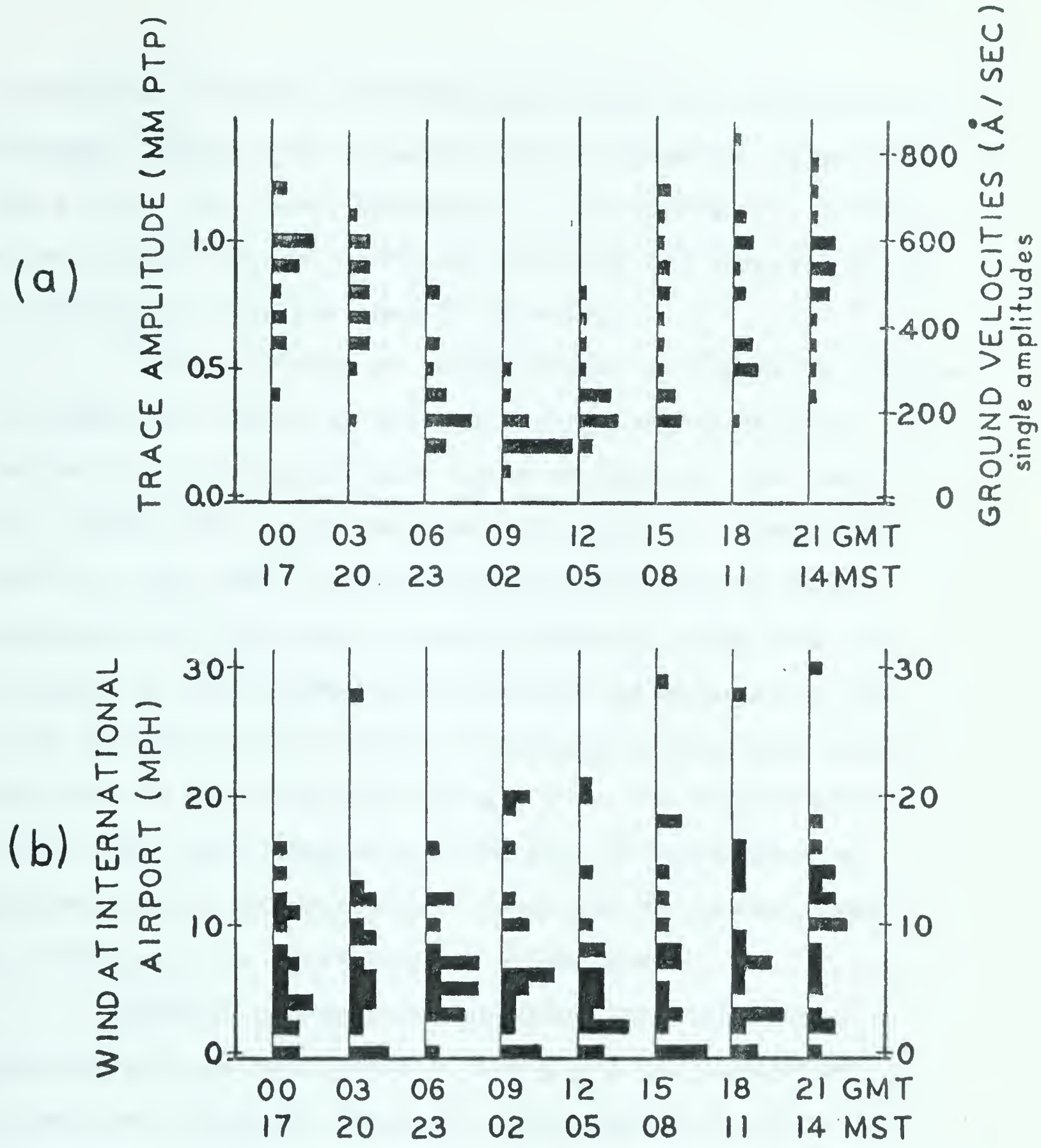


FIG. 9. June 12-30 1963, distribution of observations as a function of the time of day:

(a) U. of A. observatory SPZ 3 cps background noise

(b) Wind velocities at International Airport.

International Airport and background noise at the observatory disappear. Now, since no significant correlation appears in figure 8(a), and since assumption 1. is reasonable (the distances between the two pairs of locations are comparable) it is possible to conclude that 2. is wrong.

The conclusion is substantiated by figure 9. Figure 9(a) shows the amount by which the distribution of this observed 2 - 3 cps background noise varies with the time of day. Figure 9(b) shows that for the period of observation (June 12 - 30, 1963) no corresponding variation of wind velocities with the time of day is present. This lack of variation of wind between day and night is surprising, and may be special for the period considered, but it proves that local wind is not the main source. Even the maximum winds for each day, the velocity and the hour of occurrence of which was noted, did not seem to have had any effect that was visible on the corresponding seismograms.

Thus it has been demonstrated that the local winds are not the main cause of the 2 - 3 cps background microseisms at station Edmonton. Furthermore a clear daily variation of these microseisms has been demonstrated. This variation will be discussed further in section 5.6c.

## 5.3 Microseisms from Trans-Canada Highway

### 5.3a Introduction

This section will show that highway traffic is one of the sources of 3 cps microseisms, and some data concerning the attenuation, phase velocity and particle motion will be presented.

### 5.3b The Set-up

Figure 10 shows the location of the L-spread and of the three-component station (Z-N-E). Automobile traffic did not produce noticable 3 cps microseisms, but the very large trucks (more than ten tons) caused the microseisms to increase by a factor of ten or more.

Three such recordings were made taking note of the truck positions with respect to the numbered telephone poles shown in figure 10; the corresponding trucks will be called 1, 2, and 3. When truck 1 was passing, only four vertical seismometers were in operation ( in positions corresponding to trace 6, 7, 8, and 9 on figure 10). Truck 1 was moving fifty-four miles per hour, while trucks 2 and 3 were moving about forty miles per hour.

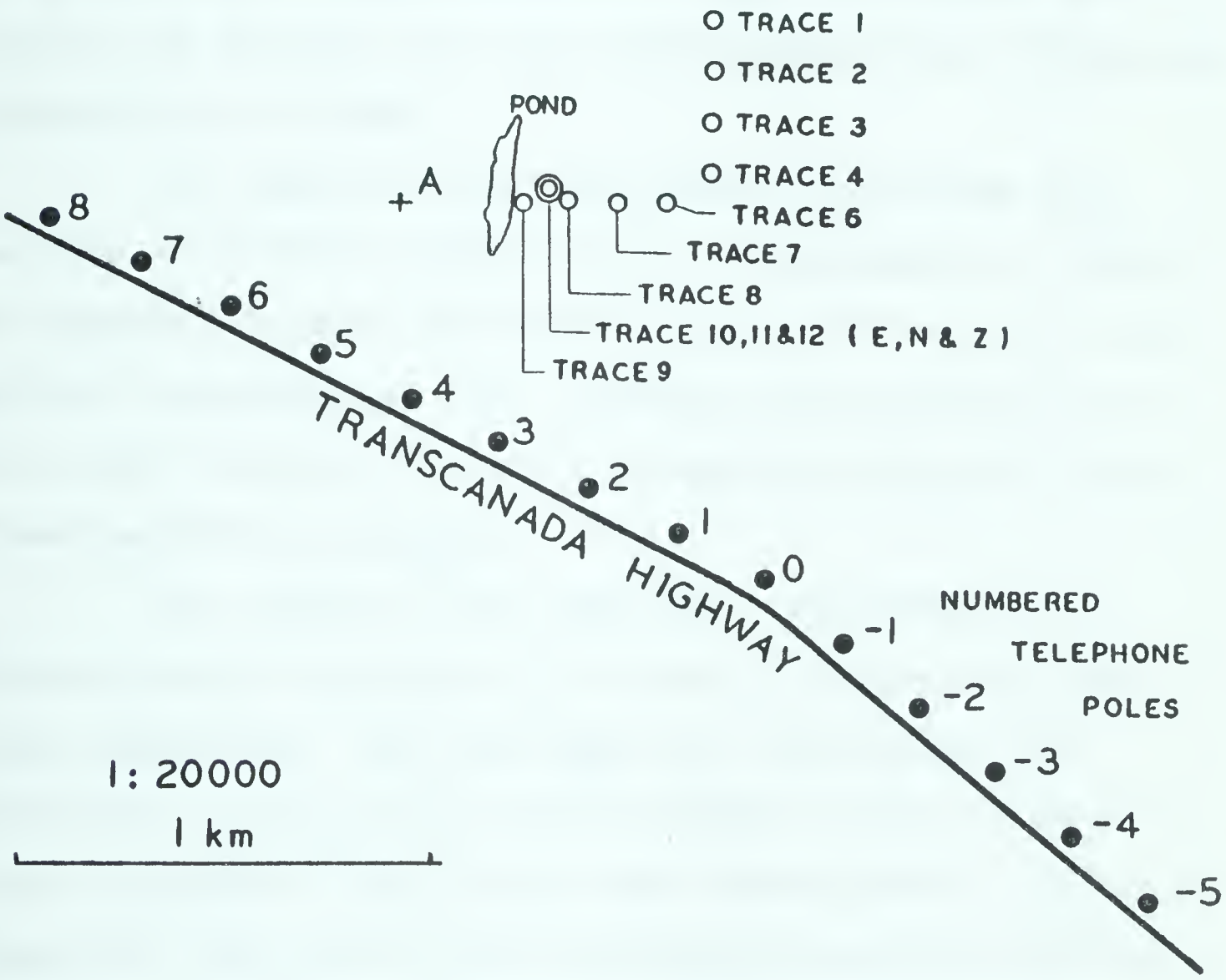


Point A is SWC, section 5, Tp 18, R12, W4.

FIG. 10.

## 5.3c The Attenuation

A number of amplitudes were measured in order to get information about the attenuation. Amplitudes from truck 1 were multiplied by .27 to make them comparable to those due to truck 2 and truck 3. This factor was arrived at by plotting the amplitudes on a logarithmic scale as a function of distance and then considering the pattern of points produced by each truck.

In figure 11 these amplitudes are plotted as a function of distance between truck and seismometer. Different symbols are used for different groups of traces to test whether the amplitudes vary smoothly with distance or if horizontal variation of elastic parameters along the setup caused amplitude anomalies.

The points in the range 650 - 750 meters on figure 11 show that traces 8, 9, and 12 consistently have larger amplitudes. In the range 800 - 1100 meters the amplitudes on trace 8, 9, and 12 differs so much, that the points encircled on the figure were investigated. It then turned out that these points correspond exactly to all the readings on traces 8, 9, and 12 originating from truck positions near pole 0 and pole 1.

Two different explanations can be offered for this effect: First, the elastic properties of the ground may possess an antinode for 3 cps vibrations, making excitation

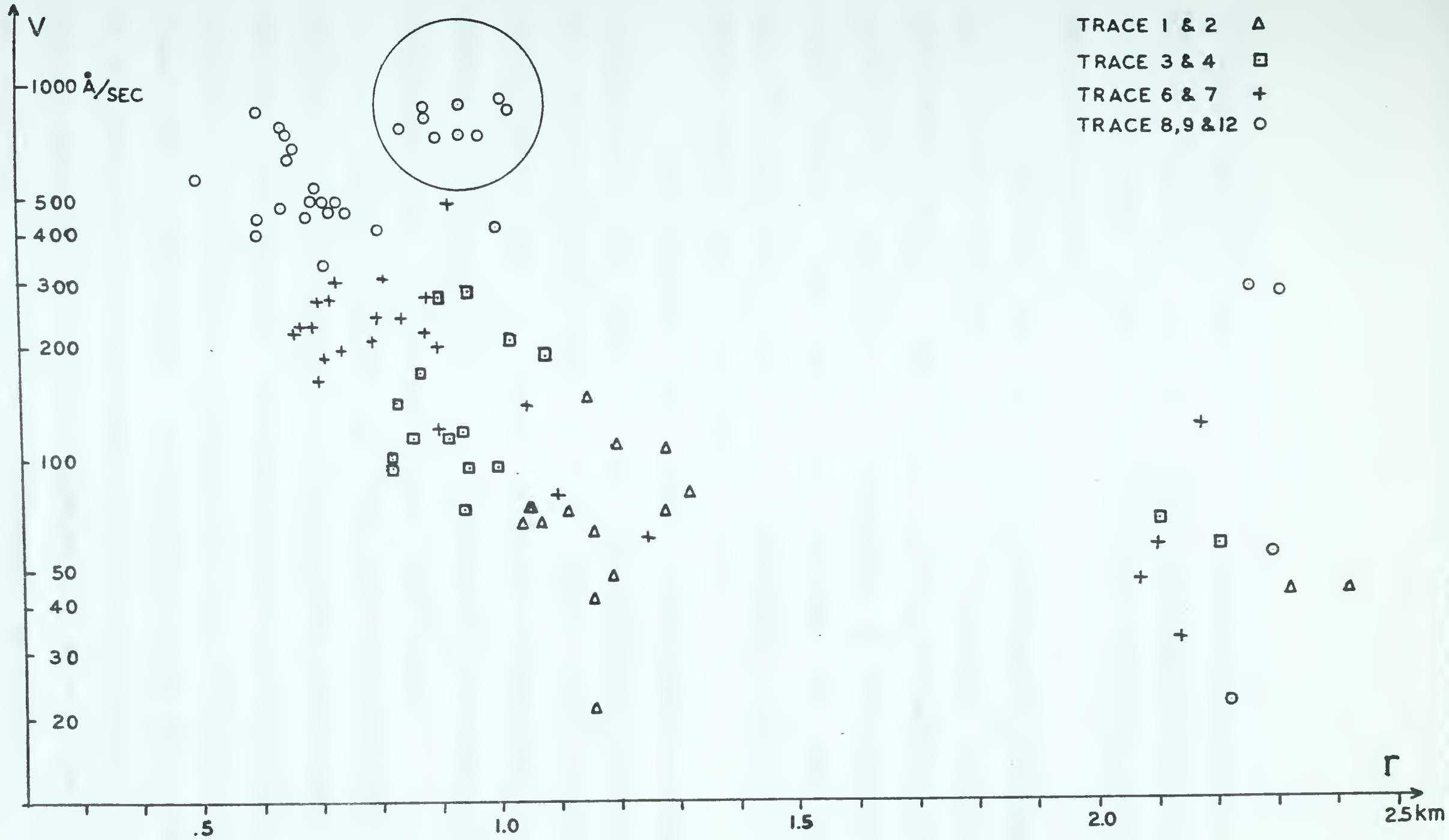


FIG. 11. Ground velocity (v) versus distance (r) from truck on Transcanada Highway.

of these vibrations more efficient. Second, the effect may simply be due to an increased noise enhancement associated with the slight change of the direction of the truck movement (see figure 10).

Whatever the cause for the increased microseisms is, it seems reasonable to reject all the values originating near poles 0 and 1. Only truck 2 and truck 3 were recorded in that area, and hence as a consequence of the rejection of the points it was found that the factor .27, used to make the amplitudes from truck 1 comparable to those of the other trucks, had to be changed to .17.

By doing this the scatter of the points was reduced considerably, and figure 12 shows the remaining points with the ordinate changed from v to $v\sqrt{r}$, where r is the distance in kilometers and v the ground velocity in Ångströms per second. A straight line on the diagram will correspond to a constant value of the attenuation coefficient $\alpha$.

Figure 12 shows that the points corresponding to traces 1, 2, 3, 4, 6, and 7 follow the same attenuation pattern, but the points corresponding to the amplitudes on traces 8, 9, and 12 are scattered at a significantly higher level (50% - 100% higher). It is worth noting that trace 8, 9, and 12 seismometers were all within 150 meters of a shallow pond while the other seismometers were on the flat and dry prairie far from any topographic anomalies.

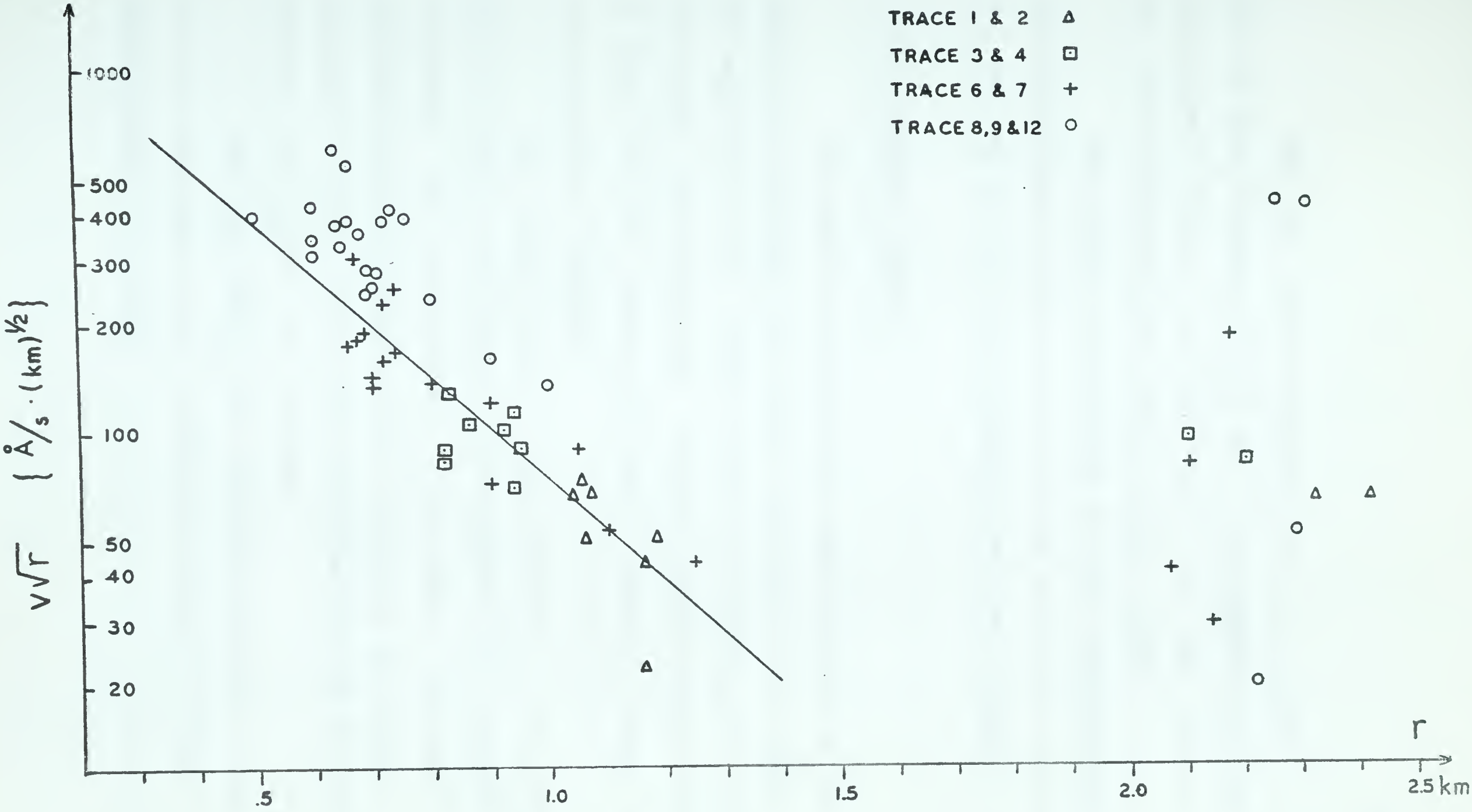


FIG. 12. v is ground velocity r is distance from truck on Transcanada Highway. The line drawn corresponds to $v\sqrt{r} \propto e^{-\alpha r}$ with $\alpha = 3.8$ . The points (o) from traces 8, 9 & 12 are ignored, being at a higher level.

The line drawn corresponds to $\alpha = 3.8\ km^{-1}$ and the mean frequency is 3.1 cps. This agrees well with Kisslinger's value, 4 to 6 $km^{-1}$ at 3.5 to 5 cps, found at the Suffield Experimental Station (Jones, 1963).

The points corresponding to truck positions more than two kilometers away do not fit the attenuation pattern, and they may be due to microseisms from other sources.

## 5.3d The Phase Velocity

In order to determine the phase velocity of the waves and investigate the spatial coherency of the waves, the velocity of wave crests in well developed groups recorded from truck 1 was determined. Similar studies using truck 2 or truck 3 did not produce meaningful results, because the waves were more irregular.

The average value for the difference $\Delta t$ of arrival times on trace 9 and trace 6 was determined for selected wavegroups. The truck position at the time of the wave generation was calculated and the difference $\Delta r$ between distances to trace 6 and trace 9 seismometers was determined. Positive and negative $\Delta r$'s occurred.

The fact that $\Delta t$ was decreasing smoothly to zero for $\Delta r$ decreasing to zero is taken as a sign that phase identification is correct.

The mean period derived from 59 measurements is 0.312 $\pm$ 0.002 seconds, and an estimate obtained for the spectral width parameter $\delta$ is 0.09.

The narrowness of the spectrum makes it reasonable to assume that the apparent wave velocity is a good estimate of the phase velocity.

Assuming a rectilinear wave propagation from the source to the receiver, $\Delta r/\Delta t$ will be an estimate of this phase velocity.

The estimate of the phase velocity obtained for truck positions between pole 4 and 7 and also for truck positions between pole 0 and 1 is 489 $\pm$ 6 m/sec. For truck positions between pole 1 and 3, however, the estimate obtained is 350 $\pm$ 50 m/sec.

The latter estimate of the standard deviation was calculated from only four observed deviations and hence it can be considered fairly uncertain. The difference between estimates of phase velocities could be due to the decrease of accuracy, when the $\Delta t$'s and $\Delta r$'s are small, but at least an apparent shift of phase velocity has been found.

### 5.3e The Particle Motion

The particle motion was studied using the modified Jensen method. Due to the low sensitivity of the Willmore

Mark I seismometer the method could only be applied to a limited number of cases. The diagrams suggested either predominantly prograde or a mixture of equal amounts of prograde and retrograde Rayleigh-type motion.

The trajectory of the particle motion for a case when the NE diagram did not show any significant trend was followed for three consecutive cycles. The particle motion was the same as would result from a refracted SV wave.* The radial amplitude was 85 Å/sec, the transverse amplitude five times less, and the vertical amplitude was 93 Å/sec.

## 5.4 Microseisms from Highway 2

### 5.4a Introduction, Comparison with Trains

In order to collect more data on the particle motion in 3 cps surface waves, some recordings were made near highway 2. The site selected was as close to the Edmonton seismic observatory site as it was possible to obtain known sources of 3 cps microseisms. These sources were trains and trucks. Comparison of the amplitudes suggests that the 3 cps energy produced by a heavy truck compares with the 3 cps energy produced by one car of a freight train, but from one car of a passenger train the energy is less. The following analysis is based on recordings of trucks.

---

* i.e. a vertically polarized S wave.

## 5.4b The Set-up, Description of the Recordings

The setup is shown in figure 13. The first three traces form a tripartite recording with a distance of 150 ft. between the seismometers. At the same location the N and E components are recorded.

Figure 14 shows a section of one of the recordings, when the corresponding truck was at position A on figure 13. The sinusoidal appearance of the oscillations is apparent, especially on traces 4 to 11.

The attenuation of the amplitude with distance is clearly visible on figure 14.

## 5.4 c The Phase Velocity

Using the same method as in section 5.3d, the phase velocity was determined from the differences of arrival times at trace 4 and trace 6 seismometers. The azimuth of the source varied from + 94° to + 50° and the results were consistent. Their mean value is $760 \pm 19$ m/sec.

On the section shown in figure 14 no phase velocities can be determined from wave correlation from the tripartite set-up on trace 1 - 3, but when the trucks were in the azimuth range + 28° to + 37°, the appearance of these traces was quite regular and the vectorial wavenumbers were deter-

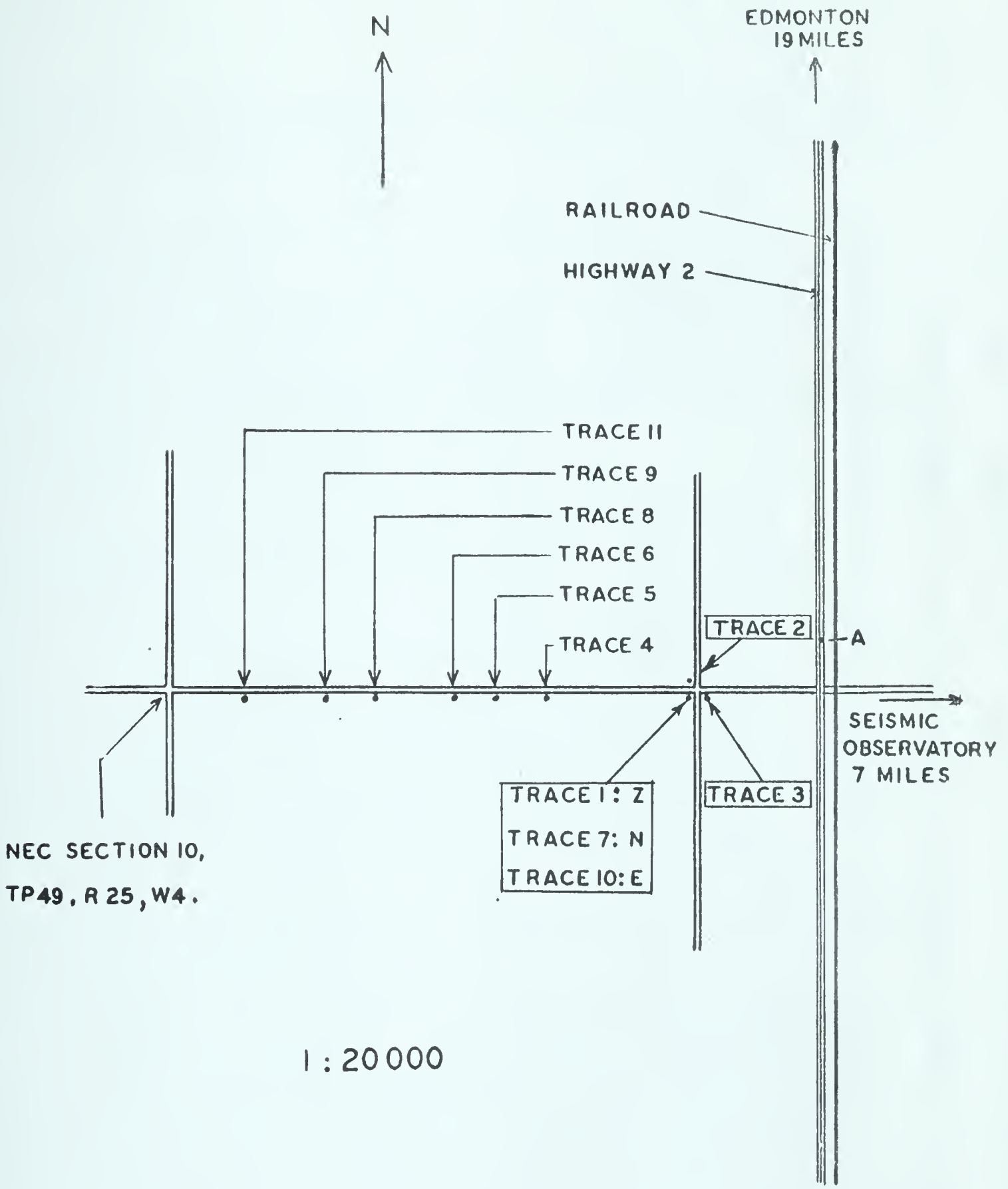


1 : 20 000

FIG. 13. Set-up near highway 2.

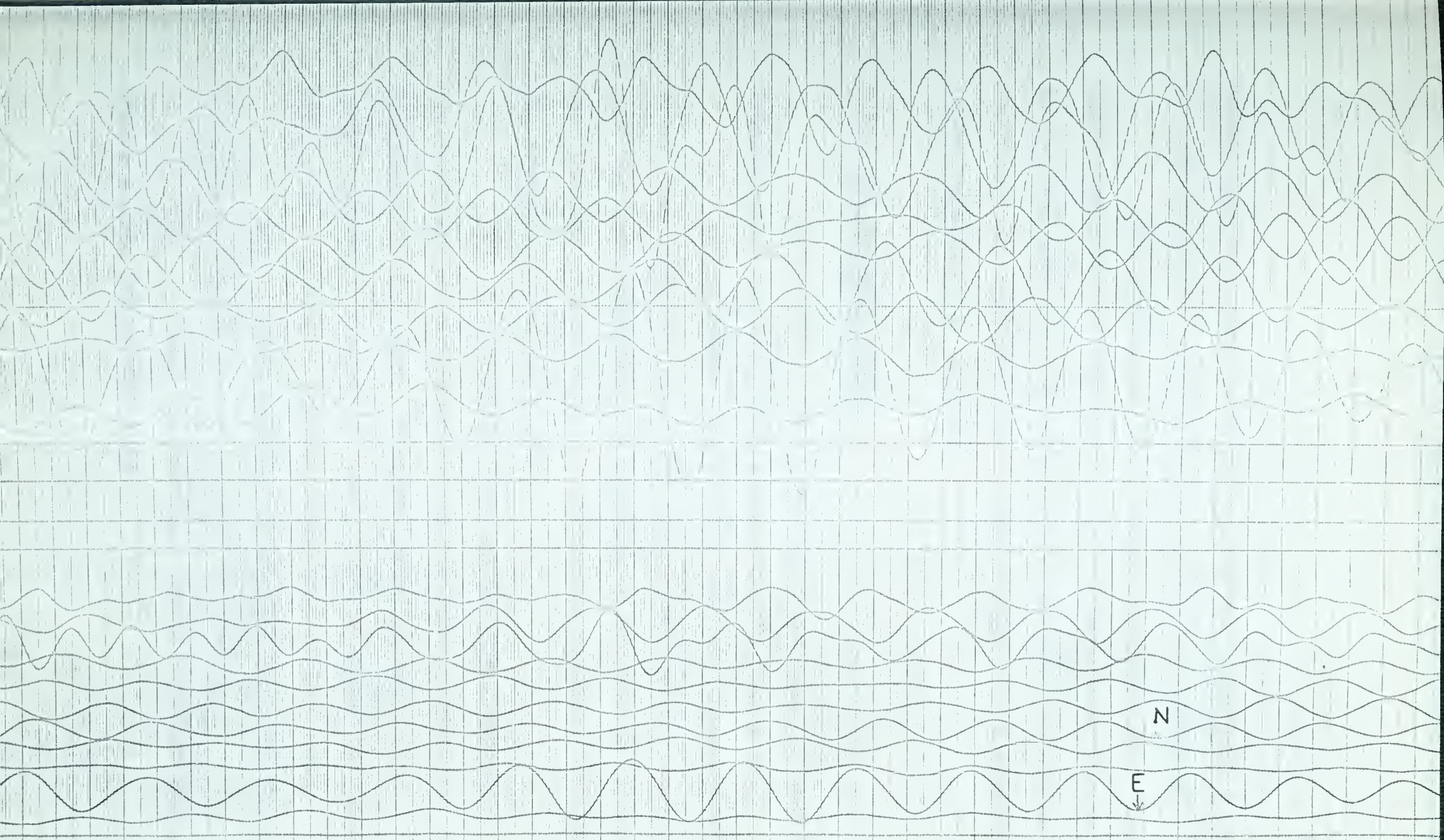


Gain of lower traces is 12 db lower than of upper traces

FIG. 14. MICROSEISMS FROM TRUCK AT POSITION "A" ON FIG. 13.

mined from the apparent velocities in the directions S and W. The vectorial wavenumbers are plotted on figure 15.

The average phase velocity determined from these wavenumbers is 880 $\pm$ 80 m/sec, but the pattern exhibited by the end points of the vectorial wavenumbers is not as expected, the pattern shows a large change of the apparent phase velocity with azimuth.

## 5.4d The Particle Motion

The particle motion was determined by the modified Jensen method and the results are shown in figure 16.

Ref. 1 shows a very clear case of prograde Rayleigh waves, the sector in which the truck moved during the time used for the measurement is opposite to the sector containing most points. The distance to the source is about 400 meters. The transverse motion is small.

Ref. 2 is derived from another truck having a similar range of positions as the one shown on Ref. 1. The conclusion is the same: Prograde Rayleigh waves with a small transverse component. Ref. 1 and 2 appear consistent with a 10 - 20 degree lateral refraction of the waves.

Ref. 3 shows dominant retrograde Rayleigh waves. The distance to the source is about 500 meters.

Ref. 4 shows dominant retrograde Rayleigh waves from a source 700 meters away.

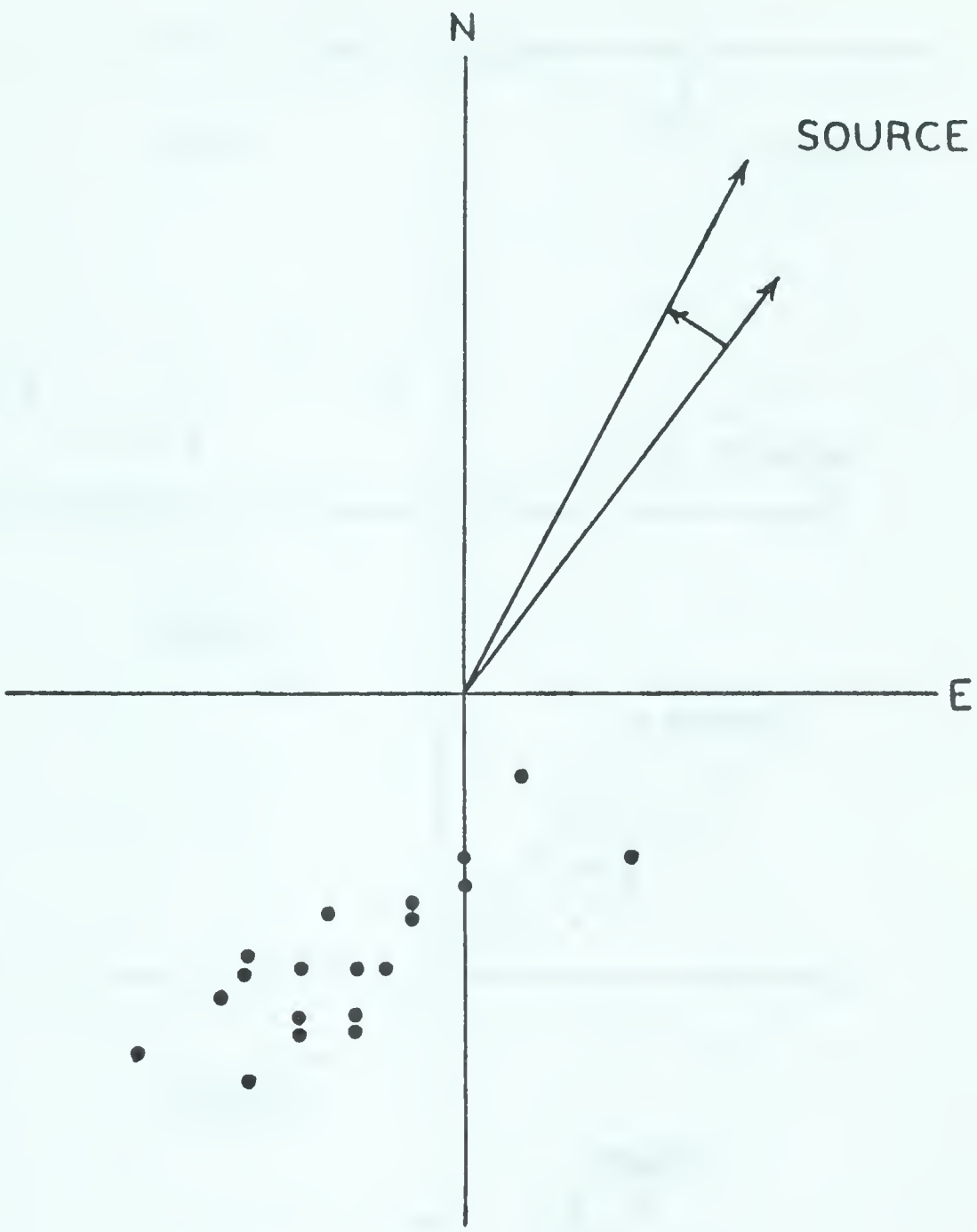


FIG. 15. Vectorial wavenumbers, determined from the tripartite set-up shown on fig. 13.

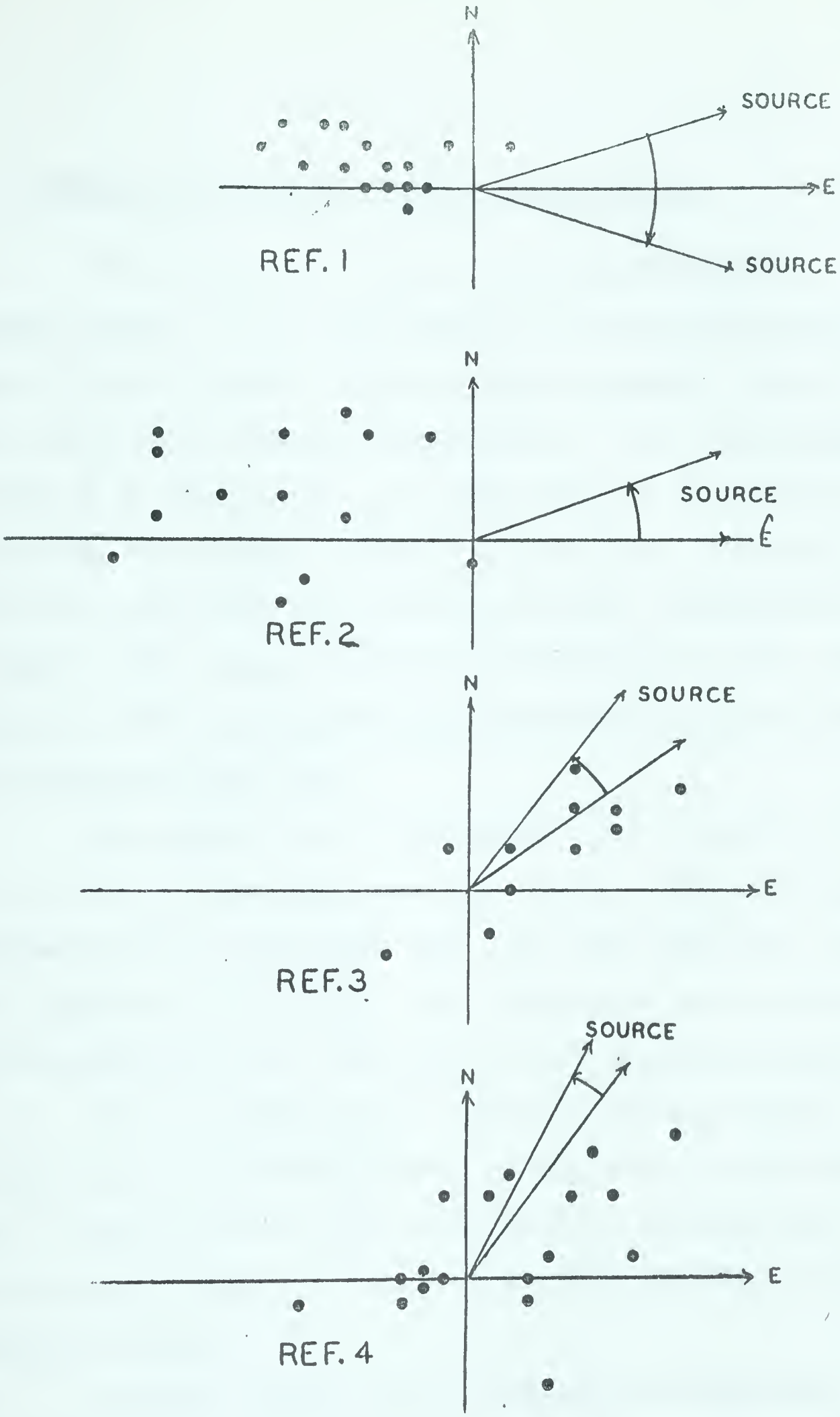


FIG. 16.

NE diagrams used to determine the particle motion of 3 cps microseisms from Highway 2. (See page 13 and page 92).

## 5.5 Regional Microseism Anomalies in Alberta

The analysis in section 5.3c demonstrated a regional anomaly of the amplitudes of 3 cps microseisms. Figure 17 shows a much larger regional anomaly. Traces 7, 8, and 9 have a maximum amplitude of 7 mm, an attenuation setting of 6, and a high cut filter setting of 8, hence from (3-15) the ground velocity is 350 Å/sec. On most other traces the amplitude is 1 mm or less which corresponds to 50 Å/sec. This anomaly cannot be explained from the topography, as the corresponding seismometers were placed in flat irrigated farm land.*

The spread was on the north line of section 33, Tp 17, R 14, W 4 one mile from Lake Newell. The trace one seismometer was on the west end. The wind speed was 16 knots, gusting to 25 knots. The appearance of the individual traces continued to be the same for all recordings made.

One recording at the shore of McGregor Lake yielded 3 cps microseisms with a ground velocity of 950 Å/sec. Two foot waves with a period of 2 seconds were observed in the lake, but shorter wavelengths were superimposed on these.

Another region, where unexplained anomalously large 3 cps amplitudes were observed, was one mile south of Brant, Tp 18, R 26, W 4. Here the winds were calm and the

---

* The 14 cps microseisms on traces 2, 3, 4, 5 is caused by an irrigation canal perpendicular to the spread.

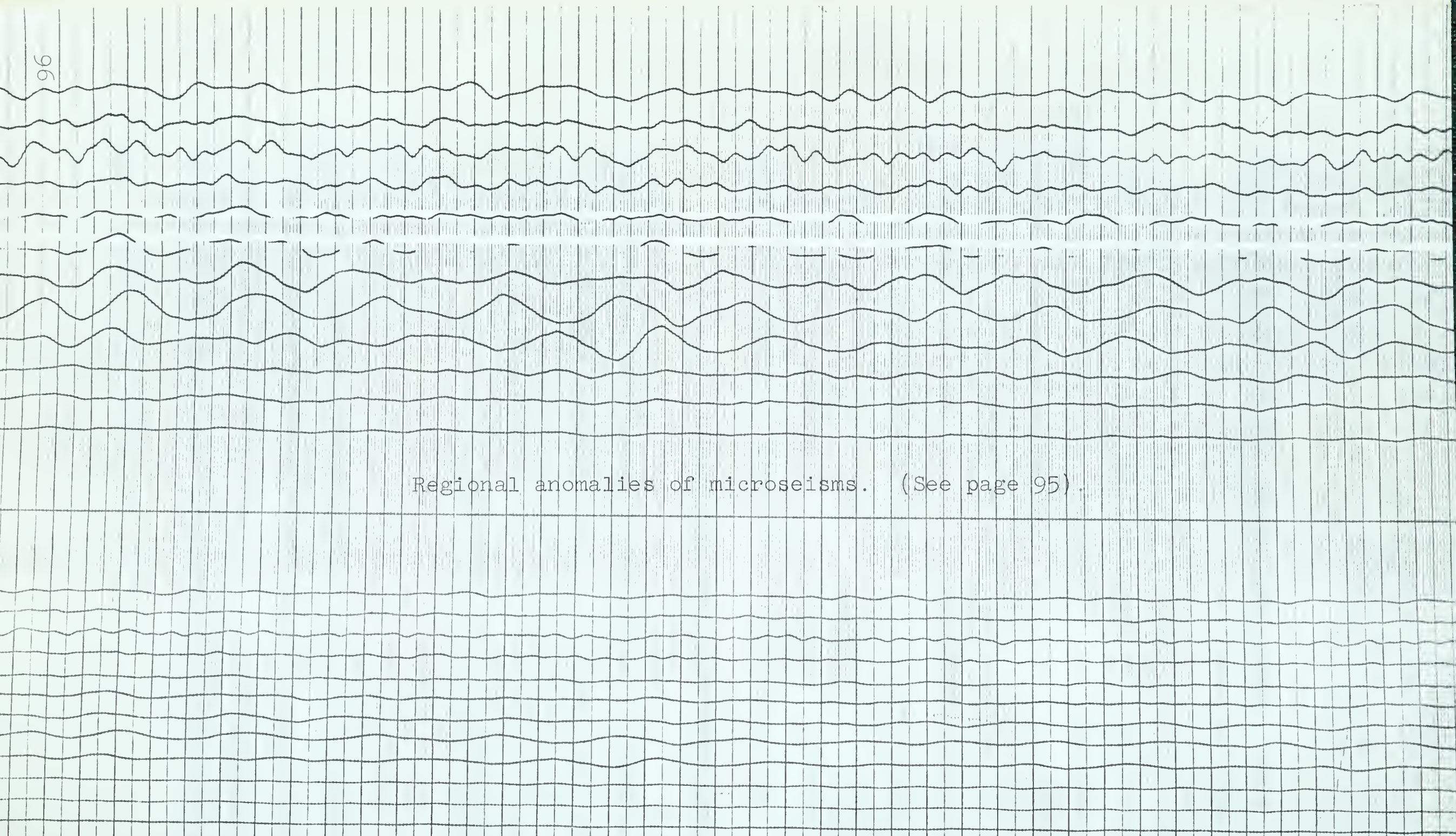

Regional anomalies of microseisms. (See page 95).

FIG. 17

amplitude variation with time was noted. The amplitude of the microseisms varied over a wide range in a few minutes time; this variation could correlate with distant highway and railroad traffic; but insufficient information is available.

## 5.6 Interpretation and Discussion

It is not possible to give a unique interpretation of all the data presented in this chapter, because often a number of different mechanisms could explain the same data.

### 5.6a Attenuation, Anomalous Propagation

The attenuation coefficient found near the Trans-Canada Highway is 3.8 $km^{-1}$ while a tentative value found near Highway 2 is 0.8 $km^{-1}$; in both cases the amplitudes would become insignificant after a few miles, and this agrees with the observations. It also explains the fact that no train microseisms could be identified on the short period seismograms obtained from station Edmonton, 7 miles from the railroad track. Assuming that the group velocities in the areas with the values $\alpha = 3.8 km^{-1}$ and $\alpha = 0.8 km^{-1}$ are 0.3 km/sec and 0.5 km/sec respectively, the corresponding Q values will be 8 and 24.

These values seem far too low to represent energy

dissipation, but they could in part be due to loss of elastic energy to more deep seated layers.

Frantti (1963) suggested that a substantial portion of the ambient high frequency earth noise originates at the earth's surface and follows a near surface propagation path.

Combining Frantti's suggestion with the Q values observed above it is suggested that 3 cps seismic energy is transferred from the surface to a near surface waveguide.

That this waveguide is near the surface was confirmed by B. Isacks (personal communication), who reported that in the recordings made by the Lamont Geological Observatory in a mine, the 1 cps component had similar amplitudes at the surface and in the mine at 2000 feet, while the 3 cps component was smaller in the mine. E. J. Douze (personal communication) using a deep well seismometer, found the 3 cps peak to disappear with depth.

The regional anomalies of 3 cps microseisms reported in section 5.5 could be due to outcroppings of this waveguide (i.e. antinodes at the surface).

An interesting example of anomalous behavior of 3 cps wave propagation was given by R. A. Page (personal communication), who kindly made copies of such seismograms available for me:

Whenever a large freight train was passing the

seismic observatory at Sterling Forest, New York, two discrete pulses of 3 cps microseisms were observed. Duration of the first pulse was about four minutes with a maximum ground velocity of 4000 Å/sec, then five minutes of usual background microseisms with amplitudes less than 1000 Å/sec and then a two minute pulse. The closest approach of the railroad track from the vault was about 6.5 km. The phenomenon is currently being studied by B. Isacks and R. Page at Lamont.

By comparison with the University of Alberta findings it is the two peaks, rather than the quiet period in between, that can be considered anomalous. These peaks could be explained by two outcroppings of the waveguide along the railroad track, and a third one at the observatory.

## 5.6b Nature of the Waves

The microseisms discussed in section 5.3 and 5.4 were not produced by air-coupled waves, because the phase velocity was considerably larger than the speed of sound.

The particle motion was most often a clear case of either retrograde Rayleigh type waves, most likely $M_1$, or prograde waves, most likely $M_2$. In a few cases the NE diagrams could be explained by a mixture of prograde and retrograde Rayleigh waves, having similar amplitudes.

In one case the particle motion could be explained by assuming refracted SV waves, but the same particle motion can be explained as interference between prograde and retrograde waves. Indeed any Lissajou figure can be explained this way: Choose a line in the plane of the particle motion. Assume that the projection of the prograde and retrograde component on this line are of equal amplitude and 180° out of phase. Then the particle motion will be rectilinear on a line perpendicular to the first. Hence by superposition of two waves the particle motion can degenerate to a line of any orientiation, and for other amplitude ratios it may become an ellipse with any inclination of the axis.

5.6c Sources of 3 cps Microseisms

Freight trains and heavy trucks were demonstrated to be sources of 3 cps microseisms. Another source of 3 cps microseisms was reported by Y. Rochard (Vesiac Staff, 1962, chapter 15) who found slightly perceptible 3 -4 cps microseisms from a stone quarry 2 km away.

Farm machinery produced a high level of 3 cps microseisms at the University of Alberta observatory, when such machinery was operating in the adjacent fields.

The measurements made near lakes disturbed by

winds suggest that some 3 cps microseisms could be produced here, but evidence is inconclusive.

An unsettled question is the nature of the source of the 2 - 3 cps background microseisms. As demonstrated in section 5.2 they show a pronounced daily variation. The attenuation pattern observed on the surface suggests that the decrease in human activities at night cannot account for this daily variation, but a stronger suggestion of non-cultural sources was obtained from P. L. Gouin (personal communication):

"The seismic observatory recordings at Addis Abeba had a high level of 1.5 - 10 cps microseisms, which invariably decreased at night by a factor of 5 or so. To filter out these disturbing microseisms the 1/4 sec. galvanometers were replaced by 2 sec. galvanometers, but the effect was still visible with a smaller trace amplitude. These microseisms could not be attributed to man-made sources; because the heavy traffic took place at night, where the microseisms were at a minimum. Neither could they be attributed to general background noise adding up from a large number of man-made sources and travelling through some waveguide; this is ruled out because in Ethiopia no industry is present and the traffic is limited to a few lines radiating from Addis Abeba.

The daytime increase occurred whether the sun was shining or not, and this increase took place within half an hour around sunrise and died out within half an hour around sunset. No striking correlation with the amplitude of the daily variation on the magnetograms were noticed".

This information gives additional support to Gherzi's inference from the Brebeuf seismograms, that some short period noise is not of cultural origin. Gouin's finding makes it doubtful that the daylight heating is the source but still makes it reasonable indirectly to suspect the sun as the source.

D. E. Smylie (personal communication) suggested tentatively that such microseisms might be due to vibrations, set up in the ionosphere by solar winds or by other electromagnetic disturbances,which then propagate with acoustic speed to the ground.

Another suggestion that some 3 cps microseisms are of atmospheric origin was given by Walsh (1955). He studied such microseisms near Saint Louis and found that they occur much more often by day than by night and that they correlate well with microbarographic activities.

## Conclusions

1. Heavy trucks and freight trains are sources of 3 cps

microseisms; at distances more than 800 meters the 3 cps peak is not disturbed by higher frequencies, but at closer range the higher frequencies occur.

2. In most cases these microseisms are damped out within a few miles, but in special cases efficient propagation for longer distances occurs.

3. These 3 cps microseisms are not aircoupled waves.

4. They contain prograde and retrograde Rayleigh type waves.

5. In two cases an apparent change of phase velocity with azimuth was observed.

6. Industry and farm machinery are sources of 3 cps microseisms.

7. The 2 - 3 cps background microseisms at station Edmonton have a clear daily variation.

8. This variation is not necessarily due to human activities; it is not due to wind, but could be of atmospheric origin.

# VI. FOUR TO FIFTY CYCLES PER SECOND MICROSEISMS

## 6.1 Introduction

A detailed study of the sources of these microseisms was not undertaken but some obvious sources were located: Machinery, traffic and wind.

## 6.2 Amplitudes

The smallest amplitudes encountered by University of Alberta were recorded near Lake Superior in a tree-covered area with the seismometers on bedrock.

Recordings of microseisms from this location were kindly supplied to me by D. Robertson. Some oscillations correlated from trace to trace and could be identified as electrical noise. Others could be either due to electrical noise or to microseisms. By treating them as microseisms it was possible to arrive at some maximum values for the ground velocities. The actual velocities may be even smaller.

Typical values were: 20 Å/sec at 5 - 10 cps, 30 Å/sec at 20 cps. These values are slightly larger than the lowest values reported by Frantti, Willis and Wilson (1962) in their survey of the amplitudes of microseisms.

## 6.3 Particle Motion

Some recordings were made at University of Alberta campus to study the particle motion in microseisms generated by machinery.

At night time it was possible to record unperturbed 7 1/2 cps microseisms generated by the University Power Plant. The particle motion was determined by the modified Jensen method. The resulting NE diagram is shown in figure 18(a) and the wave numbers determined from a tripartite setup at the same location is shown on figure 18(b).

Some lateral refraction of the waves is apparent, and their particle motion is prograde with a small transverse component. This transverse component seems to be out of phase but coupled to the vertical component, so that the same direction of transverse velocity is present whenever Z is at a maximum. This coupling may be due to the fixed position of the source and the receiver and to the periodic nature of the source. The waves cannot be called pseudo-Rayleigh waves, because the transverse and the vertical components are out of phase.

Figure 18(c) is an NE diagram from a recording of 12 cps microseisms generated by the air conditioning machine in the Physics Building. The particle motion is predominantly retrograde and the particle velocity 3800 Å/sec. This

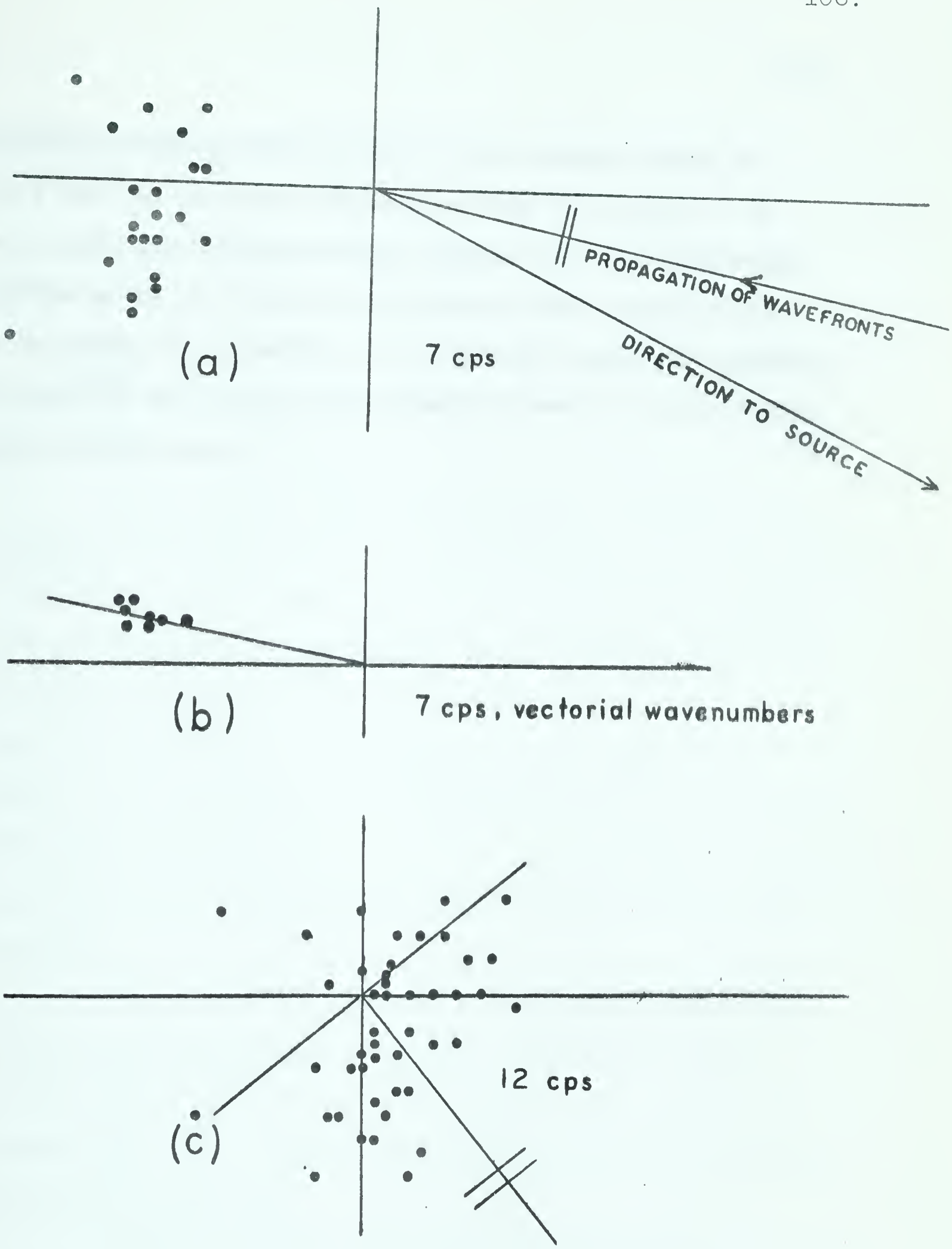


FIG. 18. NE diagrams used to determine the particle motion of 7 cps and 12 cps microseisms.

a) : prograde

c) : retrograde

See page 13 and page 105.

microseism was recorded close to the source, while the 7 1/2 cps was recorded 500 meters from the source. In both cases the particle motion agrees with Rayleigh-type surface waves, but only in the second case is the fundamental mode, $M_1$, possible. In the first case the prograde particle motion is due to $M_2$ waves (Sezawa waves) or still higher mode surface waves.

# VII. SUGGESTIONS FOR FUTURE RESEARCH

From the limitations quoted in the conclusions of chapter IV to VI many possibilities for further research are obvious; for instance more statistics about the directions of approach at Edmonton and about their dependence on the season would be of interest.

Furthermore from the discussion in section 1.2 it appears desirable to investigate ~~if~~ how often pseudo-Rayleigh waves occur. This kind of wave is a special case of a coupling between Rayleigh and Love waves, namely the case of $0^{o}$ or $180^{o}$ phase difference between the vertical and the transverse particle motion. A coupling between second mode Rayleigh and Love waves can be expected from the similarity of the dispersion curves (Oliver and Ewing, 1958a), but only in special cases would pseudo-Rayleigh waves occur by this mechanism.

If pseudo-Rayleigh waves or coupled waves with a constant phase difference not equal to $90^{o}$ occur, the particle velocity vector at times where Z has a zero-up-crossing will have a constant direction perpendicular to the direction of approach.

Consequently in cases of large p values it is suggested to read the slopes at times where Z has a zero up crossing and plot $(\frac{dN}{dt}, \frac{dE}{dt})$ in an NE diagram. If these

points, when sufficiently separated in time, fall in one direction, the Rayleigh and Love waves must be coupled. If then the angle between the line through the points and the direction of approach is significantly different from $90^{\circ}$, the waves would not be pseudo-Rayleigh waves but another kind of coupled waves. In such cases the perpendicular to the transverse motion in the half plane containing the previously determined direction of approach would be an improved estimate of the direction of approach, because if Z = 0 ~~and~~ the motion would have no longitudinal component. The improvement of the estimate is only valid, however, if the vertical component is caused by one kind of wave coming from one direction.

If the points plotted fall evenly in two directions $180^{\circ}$ apart, the transverse component must be due to uncoupled Love waves, and the best line through the points may serve the purpose of getting another estimate of the direction of approach; the indeterminacy of $180^{\circ}$ is not important once the approximate direction is known.

# BIBLIOGRAPHY

Antonenko, E. M. and Savarensky, Y. F., 1963, "O Prirodye Vўsokochastotnўkh Mikroseysm." Acad. Nauk SSSR Izv. Ser. geofiz. 3(54) pp. 81-90.

Banerji, S. K., 1930, "Microseisms Associated with Disturbed Weather in the Indian Seas." Phil. Trans. A 229 pp. 289-328.

Banerji, S. K., 1935, "Theory of Microseisms", Proc. Ind. Acad. Sci. A,1.

Barber, N. F. and Tucker, M. J., 1962, "Wind Waves", chapter 19 in "The Sea", Vol. 1, Physical Oceanography, edited by M. N. Hill, pp. 664-699, Interscience Publishers, New York.

Brune, J., 1962, "Attenuation of Dispersed Wave Trains", Seismol. Soc. America Bull. V 52, pp. 109-112.

Båth, M., 1962, "Direction of Approach of Microseisms", The Geoph. Journal V 6, pp. 450-461.

Caloi, P., 1951, "Teoria delle Onde di Rayleigh in Mezzi Elastici e firmo-elastici", Archiv. Meteorologie Geophysik u. Bioklimatologie. pp. 413-435.

Cartwright, D. E., 1958, "On Estimating the Mean Energy of Sea Waves from the Highest Waves on a Record", Proc. Roy. Soc. A. V 217, pp. 22-48.

Defant, A., 1961, "Physical Oceanography", Vol. II. Pergamon Press.

Donn, W. L., 1954, "Direction Studies Using Microseisms Ground Particle Motion", Trans. Amer. Geoph. Union. V 35, pp. 821-832.

Donn, W. L., 1957, "A Case Study Bearing on the Origin and Propagation of 2 - to 6- Second Microseisms", Trans. Amer. Geoph. Union. V 38, pp. 354-359.

Ewing, M., Jardetzky, W. S., and Press, F., 1957, "Elastic Waves in Layered Media", McGraw-Hill.

Feller, W., 1950, "An Introduction to Probabilitiy Theory and its Applications", Wiley, New York.

Frantti, G., Willis, D. E., and Wilson, James T., 1962, "The Spectrum of Seismic Noise", Seismol. Soc. Amer. Bull. V 52, pp. 113-121.

Frantti, G., 1963, "The Nature of High-Frequency Earth Noise Spectra", Geophysics, V 28, pp. 547-562.

Galbraith, J. N., 1963, "Computer Studies of Microseism Statistics with Applications to Prediction and Detection", Doctoral Dissertation, Massachusetts Institute of Technology.

Gherzi, E., 1924, "Études sur les microséismes", Notes Seism. Obs. Zi-Ka-Wei, 5.

Gherzi, E., 1962, "Some Remarks on the Type of Microseisms Recorded at Seismological Stations", Bull. de Geophysique, No. 11, College Jean de Brebenf, Montreal.

Gray, A. G., and Mathews, G. B., 1895, "Treatise on Bessel Functions".

Gutenberg, B., 1912, "Die Seismische Bodenunruhe, Gerl. Beitr. z. Geoph. V 11.

Gutenberg, B., 1921, "Untersuchungen über die Bodenunruhe mit Perioden von $4^s$ - $10^s$ in Europa", Publ. Bureau Central de l'Ass. Int. de Seismologie.

Gutenberg, B. and Van Straten, 1953 in "Symposium on Microseisms", edited by J. T. Wilson, Nat. Res. Council, Published 306, Washington.

Gutenberg, B., 1955, "Channel Waves in the Earth's Crust", Geophysics, V 20, pp. 283-294.

Gutenberg, B., 1958, "Microseisms", Advances in Geophysics, V 5.

Hald, A., 1951, "Statistical Tables and Formulas", Wiley, New York.

Hasselmann, K., 1963, "A Statistical Analysis of the Generation of Microseisms", Reviews of Geophysics, V 1, pp. 177-210.

Haubrich, R. A., Munk, W. H., and Snodgrass, F.E., 1963, "Comparative Spectra of Microseisms and Swell", Seismol. Soc. America Bull. V 53. pp. 27-37.

Hjortenberg, E., 1963, "Some Theories of Microseisms in the Light of more Recent Findings", Seismol. Soc. America Bull. V 53, pp. 1085-1090.

Jensen, H., 1958, "A Procedure for the Determination of Direction of Approach of Microseismic Waves", Geod. Inst. Medd. No. 36, Copenhagen.

Jensen, H., 1959, "Daily Determination of the Microseismic Direction in København during the IGY 1958", Geod. Inst. Medd. No. 38. Copenhagen.

Jensen, H., 1961, "Statistical Studies on the IGY Microseisms from København and Nord", Geod. Inst. Medd. No. 39 Copenhagen.

Jones, G. H. S., 1963, "Strong Motion Seismic Effects of the Suffield Explosions", Doctoral Dissertation, University of Alberta.

Kanai, K., 1955, "On Sezawa waves ($M_2$-waves)", Part II, Bull. Earthq. Res. Inst., Tokyo Univ. V 33, pp. 275-281.

Kisslinger, C., 1959, "Observations of the Development of Rayleigh-type Waves in the Vicinity of Small Explosions", Journ. of Geoph. Res. V 64, pp. 429-436.

Knopoff, L. and MacDonald, J. F., 1958, "Attenuation of Small Amplitude Stress Waves in Solids", Reviews of Modern Physics, V 30, pp. 1178-1192.

Knopoff, L., 1959, "The Seismic Pulse in Materials Possessing Solid Friction, II: Lamb's Problem", Seismol. Soc. America, V 49, pp. 403-413.

Lee, A. W., 1932, "The Effect of Geological Structure upon Microseismic Disturbance", M.N.R.A. Soc. Geophys. Suppl., 3, pp. 83-105.

Lee, A. S., 1934, "Further Investigations of the Effect of Geological Structure upon Microseismic Disturbance", M.N.R.A. Soc. Geophys. Suppl. 3.6.

Lehmann, I. and Ewing, M., 1960, "On Short-Period Surface Waves as Recorded in Copenhagen", Geod. Inst. Skrifter 3. Rk., Bd. 34, Copenhagen.

Longuet-Higgins, M. S., 1950, "A Theory of the Origin of Microseisms", Phil. Trans. Roy. Soc. of London A. V 243, pp. 1-35.

Longuet-Higgins, M. S., 1957, "The Statistical Analysis of a Random Moving Surface", Phil. Trans. Roy. Soc. of London, A. V 249.

McDonal, F. J. et al., 1958, "Attenuation of Shear and Compressional Waves in Pierre Shale" Geophysics, V 23, pp. 421-439.

Monakhov, F. I. and Dolbilkina, N. A., 1958, "The Structure of Microseisms", Bull. Izvest. Acad. Nauk. USSR. Geoph. Ser. pp. 537-541. (english edition by Amer. Geoph. Union)

Nagamune, T., 1956, "$M_2$ Waves in a Medium with Double Surface Layers", Geoph. Mag. Tokyo, V 27, pp. 345-352.

Oliver, J. and Ewing, M., 1957, "Higher Modes of Continental Rayleigh Waves", Seismol. Soc. America, Bull. V 47, pp. 187-204.

Oliver, J. and Ewing M., 1958a, "Normal Modes of Continental Surface Waves", Seismol. Soc. America, Bull. V 48, pp. 33-49.

Oliver, J. and Ewing, M., 1958b, "The Effect of Surficial Sedimentary Layers on Continental Surface Waves", Seismol. Soc. America Bull., V 48, pp. 339-354.

Oliver, J., 1962, "A Summary of Observed Seismic Wave Dispersion", Seismol. Soc. America, Bull., V 52, pp. 81-86.

Press, F. and Ewing, M., 1948, "A Theory of Microseisms with Geologic Applications", Trans. Amer. Geoph. Union, V 29, pp. 163-174.

Rice, S. O., 1944, "Mathematical Analysis of Random Noise", Bell Syst. Technical Journal, V 25, reprinted as
Rice, S. O., 1954, in Wax, N., Selected Papers on Noise and Stochastic Processes, Dover.

Sezawa, K. and Kanai, K., 1935, "Discontinuity in the Dispersion Curves of Rayleigh Waves", Bull. Earthq. Res. Inst. Tokyo Univ., V 13, pp. 237-244.

Sezawa, K. and Kanai, K., 1940, "Dispersive Rayleigh-waves of Positive or Negative Orbital Motion, and Allied Problems", Bull. Earthq. Res. Inst. Tokyo Univ. V 18, pp. 1-9.

Suzuki, T., 1933, "Amplitude of Rayleigh Waves on the Surface", Bull. Earthq. Res. Inst. Tokyo Univ. V 11, pp. 187-195.

Tolstoy, I. and Usdin, E., 1953, "Dispersive Properties of Stratified Elastic and Liquid Media: A Ray Theory", Geophysics, V 18, pp. 844-870.

Vesiac Staff, 1962, "Problems in Seismic Background Noise", Acoustics and Seismic Laboratory, Institute of Science and Technology, The University of Michigan, Ann Arbor.

Walsh, D. H., 1955, "An Observational Study of the Origin of Short-Period Microseisms near Saint Louis, Missouri", Trans. Amer. Geoph. Union, V 36, pp. 679-687.

Weaver, D., 1962, "Crustal Studies in Southern Alberta", Masters' Thesis, University of Alberta.

Wiechert, E., 1905, "Verhandl der 2ten Intern. Seis. Konf." Gerl. Beitr. z. Geoph. Ergänzungsband 2, pp. 41-42.

Willis, D. E. and Wilson, James T., 1960, "Maximum Vertical Ground Displacement of Seismic Waves Generated by Explosive Blasts", Seismol. Soc. America Bull. V 50, pp. 455-459.

Wilson, C. D. V., 1953a, "The Origin and Nature of Microseisms in the Frequency Range 4 to 100 c/s", Proc. Roy. Soc. London A 217, pp. 176-188.

Wilson, C. D. V., 1953b, "An Analysis of the Vibrations Emitted by Some Man-made Sources of Microseisms", Proc. Roy. Soc. London, A 217, pp. 188-202.

Yamagushi, R. and Sato, Y., 1955, "Range of Possible Existence of Rayleigh and Sezawa Waves in a Stratified Medium", Bull. Earthq. Res. Inst. Tokyo Univ. V 33.3.

# APPENDIX A

# RAYLEIGH WAVES IN A SOLID LAYER OVER A SOLID HALF SPACE

## A.1 General Discussion

While the theory of Rayleigh waves in a homogeneous, isotropic and solid half space is rather simple, there is a considerable increase in algebraic difficulties whenever an additional horizontal layer is added to the model. Consequently most calculations are performed on a two layer case, i.e. a model consisting of a homogeneous, isotropic and solid half space in welded contact with a homogeneous, isotropic and solid layer of constant thickness. In this appendix only two layer cases will be considered; the primed quantities will refer to the superficial layer and the unprimed quantities will refer to the half space.

The following symbols will be used:

$L$ = wavelength

$k$ = wave number = $2\pi/L$

$H$ = layer thickness

$v_s$ = S-wave velocity

$\lambda, \mu$ = Lame's elastic parameters, $\mu$ = rigidity

$\rho$ = density

$C_R$ = Rayleigh wave velocity in a half space

"'" refers to upper medium .

By solving the period equation (e.g. Ewing, Jardetzky and Press, 1957, p. 191) derived from the boundary conditions on the surface and the interface it is possible to calculate the phase velocity as a function of the dimensionless parameter kH. Several solutions are possible, corresponding to different modes. Among these only the fundamental Rayleigh mode will have a phase velocity that approaches $C_R'$ when $kH \to \infty$. The phase velocities in the other modes will in general approach $v_s'$ for $kH \to \infty$.

If the rather stringent condition for the existence of Stoneley waves is satisfied, there will be an additional mode for which the phase velocity approaches the speed of Stoneley waves as $kH \to \infty$. The condition for the existence of Stoneley waves is shown by Ewing, Jardetzky and Press (1957, p. 113) for two different cases; the condition is that the difference between the S wave velocities $v_s$ and $v_s'$ is fairly small.

An infinity of additional modes exists with phase velocities approaching $v_s'$ when $kH \to \infty$. These are the higher shear modes, each of which has a cutoff frequency, corresponding to a least value of kH. Below this cutoff frequency unattenuated propagation does not occur.

The higher shear modes are numbered so that the first shear mode in general has the lowest cutoff frequency and the lowest phase velocities. At the cutoff frequency

the phase velocity is equal to $v_s$.

In the model computed by Tolstoy and Usdin (1953, p. 860) the first three shear modes are computed by the method of ray superposition; in their notation the first three shear modes are $M_{21}$, $M_{12}$, and $M_{22}$. The distinction between the modes $M_{1n}$ and $M_{2n}$ originates from the theory of vibrations in elastic plates, where $M_{1n}$ corresponds to the symmetric and $M_{2n}$ to the antisymmetric vibrations. According to J. Oliver and L. R. Sykes (personal communication) this distinction is not convenient for waves in a layered half space, and the waves are far from being either symmetric or antisymmetric.

In the model used by Tolstoy and Usdin, the $M_{21}$ is the first shear mode; this mode is called $M_2$ by many authors, including Oliver and Ewing (1957). The question of the nomenclature of the higher mode Rayleigh waves is not settled, however; sometimes the numbering of the shear modes is arbitary when phase velocity curves intersect. A classification based on the number of nodal planes for the horizontal or vertical motion is not immediately recommendable, because no general simple rule is known that gives the number of such nodal planes in a given shear mode. In the fundamental Rayleigh mode there is one nodal plane for horizontal motion and no nodal plane for the vertical motion.

## A.2 Particle Motion and Rayleigh's Constant as an Exploration Tool

As mentioned in section 1.2 prograde particle motion on the surface will, in the $M_2$ mode, usually be associated with a large ratio $\mu/\mu'$, while smaller ratios will be associated with retrograde motion. When prograde particle motion is observed, it can be concluded that the mode observed is not the fundamental Rayleigh mode. Assuming the mode to be $M_2$, it can then be concluded that the ratio $\mu/\mu'$ is rather large. Further conclusions can be reached by considering the Rayleigh's constant, i.e. the horizontal amplitude divided by the vertical amplitude. For convenience we will define the Rayleigh constant to be positive for retrograde and negative for prograde particle motion.

Lee (1932 and 1934) suggested that Rayleigh's constant provides a useful tool to get information about the superficial layers of softer sediments. Since this information can be deduced without knowing the distance to the source, the microseisms may provide the Rayleigh waves needed.

The Rayleigh constants for $M_1$ and $M_2$ waves will both be functions of $L/H$, $\mu/\mu'$, $\rho/\rho'$. In general the variation of the rigidity contrast is much larger than the variation of the density contrast, and in the models chosen

by different authors the density contrast $\rho/\rho'$ has always been close to 1 while the rigidity contrast $\mu/\mu'$ has varied between 2 and $\infty$. Table V shows some values of Rayleigh's constant for the $M_1$ mode while Table VI shows some values of this constant for the $M_2$ mode. Not all the values given originate from just one source: 3 points of Sezawa and Kanai's (1940) calculations agreed well with the curves given by Suzuki (1933), and Oliver and Ewing (1957) checked 3 of their results against Kanai's earlier values, calculated with the same parameters.

The usefulness of Rayleigh's constant as a tool to obtain information about parameters of crustal layers was questioned by Banerji, who wrote that Lee's analysis for layers that are of extent small in comparison with the wavelength of the Rayleigh waves appear to be unsound. The validity of Banerji's objection will depend on the layer thickness and on the rigidity contrast. As Table V shows, a rigidity contrast of 1:5 and a wavelength 20 times the layer thickness will give a Rayleigh constant of 0.99, which is appreciably higher than the value 0.68 approached for $\frac{L}{H} \rightarrow \infty$.

Since the Rayleigh constant depends on many parameters, and since a two layer model is not always detailed enough to explain experimental data, the Rayleigh constant alone will provide very incomplete information about crustal structure; it may provide the check, however,

TABLE V

Rayleigh's Constant in the $M_1$ Mode with Poisson's condition satisfied in both media.

| Source of information | $\rho/\rho'$ | $\mu/\mu'$ | L/H | Rayleigh's constant |
|---|---|---|---|---|
| Suzuki (1933) | 1 | 2 | 1 | 0.67 |
| | 1 | 2 | 2 | 0.76 |
| | 1 | 2 | 15 | 0.81 |
| | 1 | 2 | 20 | 0.78 |
| | 1 | 4 | 1 | 0.67 |
| | 1 | 4 | 2 | 0.70 |
| | 1 | 4 | 9 | 1.14 |
| | 1 | 4 | 20 | 0.96 |
| | 1 | 5 | 1 | 0.67 |
| | 1 | 5 | 3 | 0.48 |
| | 1 | 5 | 6 | 1.19 |
| | 1 | 5 | 8 | 1.30 |
| | 1 | 5 | 20 | 0.99 |
| Sezawa and Kanai (1940) | 1 | 20 | 2 | 0.64 |
| | 1 | 20 | 5 | 2.00 |
| | 1 | 20 | 16 | 2.63 |
| | 1 | ∞ | 2 | 0.59 |
| | 1 | ∞ | 6 | 0.34 |
| | 1 | ∞ | 9 | 0.23 |

Model:

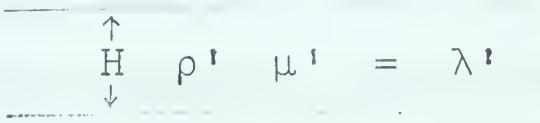

TABLE VI

Rayleigh's Constant in the $M_2$ Mode with Poisson's Condition Satisfied in both Media.

| Source of information | $\rho/\rho'$ | $\mu/\mu'$ | L/H | Rayleigh's Constant |
|---|---|---|---|---|
| Oliver and Ewing (1957) | 1.11 | 2.09 | 0.49 | 0.55 |
| | 1.11 | 2.09 | 0.81 | 0.44 |
| | 1.11 | 2.09 | 1.56 | 0.14 |
| | 1.11 | 2.09 | 2.64 | 0.10 |
| | 1 | 8 | 0.628 | 0.51 |
| | 1 | 8 | 1.066 | 0.17 |
| | 1 | 8 | 1.29 | -0.20 |
| | 1 | 8 | 1.62 | -0.91 |
| | 1 | 8 | 2.44 | -2.32 |
| | 1 | 8 | 3.76 | -2.02 |
| | 1 | 8 | 4.94 | -1.01 |
| | 1 | 8 | 7.15 | -0.77 |
| Sezawa and Kanai (1940) | 1 | 5 | 1.7 | -3.82 |
| | 1 | 5 | 3.3 | -1.64 |
| | 1 | 5 | 5.2 | -0.98 |
| | 1 | 20 | 2.7 | -3.14 |
| | 1 | 20 | 5.0 | -0.39 |
| | 1 | 20 | 13.2 | -0.99 |
| | 1 | $\infty$ | 2.0 | -2.0 |
| | 1 | $\infty$ | 6.0 | -9.6 |
| | 1 | $\infty$ | 9.0 | -14.8 |

Positive Rayleigh constant means retrograde particle motion.

Negative Rayleigh constant means prograde particle motion.

on a structure obtained by other means, and the value of this check will increase if it is possible to determine the Rayleigh constant for a range of different frequencies.

The fact that the Rayleigh constant is sensitive to a superficial layer of sediments was used by Oliver and Ewing (1957) to explain a discrepancy between the observed Rayleigh constant and the one predicted from a two layered model.

## A.3 Necessary Conditions for Sezawa Waves to Exist

In section A.1 it was pointed out that for $M_2$ waves a cut off frequency exists corresponding to a minimum value of kH, i.e. a maximum value of L/H. This maximum value can be expressed as a function of $\mu/\mu'$ and $v_s/v_s'$. This function was calculated by Yamaguchi and Sato (1955) and their results are shown on figure 19. To convert the wavelength L used in the figure, into frequency, a knowledge of the phase velocity $C_{M2}$ of the $M_2$ waves is necessary. An exact value of this may be obtained from the dispersion curves (e.g. Sezawa and Kanai, 1935) or, if applicable, from one of the published dispersion curves for $M_2$-waves. An approximate value, however, may be derived from the following information, given by Kanai (1955):

1° When the conditions for the existence of Stoneley waves is satisfied:

$$v_{Stoneley} < C_{M2} < v_s$$

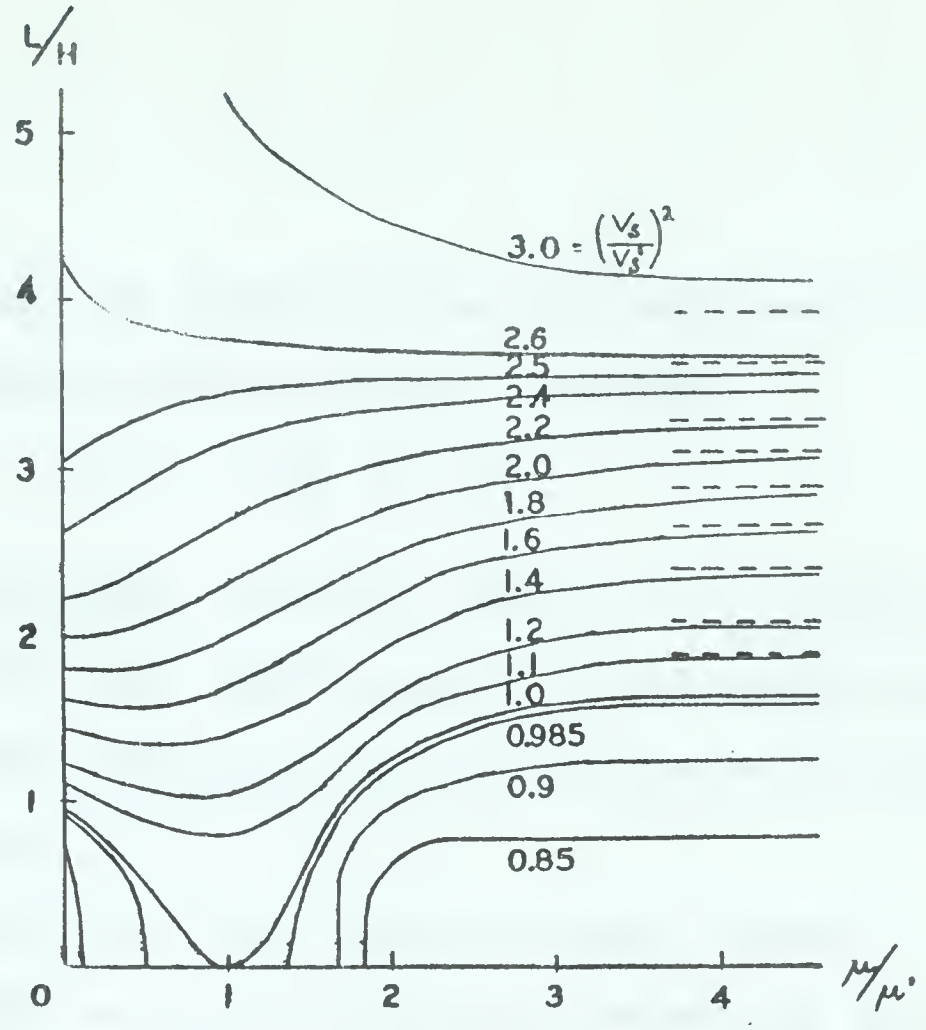


MODEL :

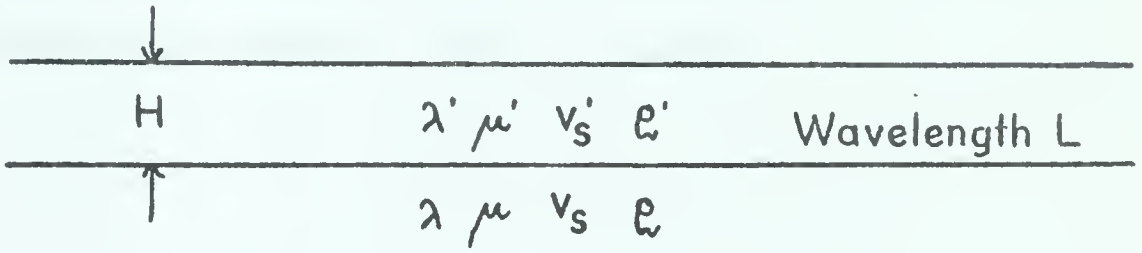


$\lambda' = \mu' \quad \lambda = \mu$ (Poisson's condition)

FIG. 19. Critical curves that for given $\left(\frac{V_S}{V_S'}\right)^2$ divides the diagram into two regions, the upper one, where only $M_1$ Rayleigh waves can exist, and the lower one, where both $M_1$ and $M_2$ waves are allowed to exist.

When $\left(\frac{V_S}{V_S'}\right)^2 < 0.8456$ $M_2$ waves cannot exist.

*(After Yamaguchi and Satô)*

2° When the condition for the existence of Stoneley waves is not satisfied:

$$v_s' < C_{M2} < v_s$$

The implication from 2°, that $v_s' < v_s$, is in accordance with the fact that $M_2$ waves do not exist for $v_s' > v_s$ unless the conditions for the existence of Stoneley waves is satisfied.

The velocity of the Stoneley wave, quoted in 1° "falls between the velocity of Rayleigh waves and that of transverse waves in the medium of greater acoustic velocity" (Ewing, Jardetzky, and Press, 1957, p. 112).